A SHERLOCK toolbox for eco-epidemiological surveillance of African trypanosomes in domestic pigs from Western Africa.

Roger-Junior Eloiflin*[1], Elena Pérez-Antón*[2], Aïssata Camara*[3], Annick Dujeancourt-Henry[2], Salimatou Boiro[3], Martial N'Djetchi[4], Mélika Taoré[4], Mathurin Koffi[4], Dramane Kaba[5], , Yann Le Pennec[6], Bakary Doukouré[6], Abdoulaye Dansy Camara[7], Moïse Kagbadouno[7], Pascal Campagne[8], Mamadou Camara[7], Vincent Jamonneau[1], Sophie Thevenon[1,9], Jean-Mathieu Bart[1,7], Lucy Glover[2,#], and Brice Rotureau[3,10,#]

[1] INTERTRYP, Université de Montpellier, Cirad, IRD, Montpellier, France

[2] Trypanosome Molecular Biology Unit, Institut Pasteur, Université de Paris, INSERM U1347, Paris, France

[3] Parasitology Unit, Institut Pasteur of Guinea, Conakry, Guinea

[4] Unité de Formation et de Recherche Environnement, Université Jean Lorougnon Guédé, Daloa, Côte d'Ivoire

[5] Unité de Recherche Trypanosomoses, Institut Pierre Richet, Bouaké, Côte d'Ivoire

[6] Virology Unit, Institut Pasteur of Guinea, Conakry, Guinea

[7] Programme National de Lutte contre la Trypanosomiase Humaine Africaine, Ministère de la Santé, Conakry, Guinea

[8] Bioinformatics and biostatistics hub, Institut Pasteur, Paris, France

[9] Cirad, UMR INTERTRYP, Montpellier, France

[10] Trypanosome Transmission Group, Trypanosome Cell Biology Unit, Institut Pasteur, Université Paris Cité, INSERM U1347, Paris, France

* Equal contributions

[#] Corresponding authors: Brice Rotureau, rotureau@pasteur.fr; Lucy Glover, lucy.glover@pasteur.fr

Short title

A SHERLOCK toolbox for AAT surveillance

Abstract

Animal African trypanosomosis (AAT), caused by protist parasites of the genus *Trypanosoma,* puts upward of a million head of livestock at risk across 37 countries in Africa. The economic impact of AAT and the presence of human-infectious trypanosomes in animals place a clear importance on improving diagnostics for animal trypanosomes to map the distribution of the veterinary parasites and identify reservoirs of human-infectious trypanosomes. We have adapted the CRISPR-based detection toolkit SHERLOCK (Specific High-sensitivity Enzymatic Reporter unLOCKing) for trypanosomatid parasites responsible for AAT (SHERLOCK4AAT) including Pan-trypanosomatid, *Trypanozoon*, *T. vivax*, *T. congolense*, *T. theileri*, *T. simiae* and *T. suis* assays. To test the applicability of this technique in the field, we analysed dried blood spots collected from 200 farm and 224 free-ranging pigs in endemic and historical human African trypanosomiasis foci in Guinea and Côte d'Ivoire, respectively. The results revealed that SHERLOCK4AAT can detect and discriminate between trypanosome species involved in multiple infections with a high sensitivity. 62.7 % [58.1, 67.3] of pigs were found infected with at least one trypanosome species. *T. brucei gambiense*, a human-infectious trypanosome, was found in one animal at both sites, highlighting the risk that these animals may act as persistent reservoirs. These data suggest that, due to their proximity to humans and their attractiveness to tsetse flies, pigs could act as sentinels to monitor *T. b. gambiense* circulation using the SHERLOCK4AAT toolbox.

Introduction

Through a combination of vector control, reactive screening, passive diagnosis, new therapeutic drugs and the support of national control programmes, donors and stakeholders, interrupting the transmission of gambiense human African trypanosomiasis (HAT) at pan-African level is in reach (***Barrett et al., 2024***). Reported annual cases have been maintained below 1,000 since 2018, making the elimination (zero transmission) of gambiense HAT (gHAT) by 2030, one of the major objectives of the World Health Organisation (WHO), achievable (***Franco et al., 2024***). Nevertheless, animal African trypanosomosis (AAT), also known as *nagana*, remains a significant

burden to sustainable agricultural development, and represents a threat to livestock and small holder economies (***Boulangé et al., 2022***), with a total estimated loss of 4.75 billion USD per year in terms of agricultural gross domestic product in tsetse-infested lands (***Budd, 2001***). Unlike HAT, that is caused by either *Trypanosoma brucei (T. b.) gambiense* in West Africa, or *T. b. rhodesiense* in East Africa, AAT encompasses a wider range of trypanosomatid parasites. In sub-Saharan Africa, animal infecting trypanosomes including *T. vivax*, *T. congolense*, *T. brucei*, *T. theileri*, *T. simiae* and *T. suis* are transmitted by blood-sucking flies, such as Glossinidae and Tabanidae, to a wide range of wild and domestic mammals. Socio-environmental factors such as land cover, humidity, temperature and livestock migration impact trypanosome transmission (***Karshima et al., 2016***). This is particularly evident in rural areas of sub-Saharan Africa, where high incidences of *T. brucei*, *T. congolense* and *T. vivax* are observed, due to conditions favourable to the proliferation of flies (***Okello et al., 2022b***).

Symptoms of AAT are host and pathogen-dependent, with an infection potentially leading to spontaneous abortions, reduction in milk and meat production, delays in sexual maturity, low calving rates, loss of draught power, and ultimately to high mortality, all of which compound poverty in many Sub-Saharan countries (***Kristjanson et al., 1999***). Indirect control strategies including the combination of vector control, breeding of trypanotolerant animals, and avoiding grazing in infested areas have proved to be efficient in reducing the number of infections (***Meyer et al., 2016***). Chemotherapy and chemoprophylaxis are the main means for controlling AAT, although inadequate usage, presence of fake drugs and emergent drug resistance are hampering trypanocide efficacy (***Giordani et al., 2016; Richards et al., 2021***). Reliable and adapted diagnostic tests are crucial for parasite detection to better target infected animals for treatment, as well as for parasite identification to understand the distribution of trypanosomes in endemic areas. Microscopic, serological and molecular methods are generally used to diagnose AAT. Microscopy based methods are the most commonly used diagnostic methods, but lack sensitivity with a limit of detection (LoD) ranging from 10^4 to 10^5 parasites/mL when using fresh blood, to 250 to 5,000 parasites/mL for methods combining centrifugation (***Desquesnes et al., 2022a***). Serological methods, such as the card agglutination test (CATT) and ELISA, can be used to identify anti-*Trypanosoma* antibodies, but their reliability is often compromised

93 by the poor antigen characterization in animal infecting trypanosomes or by the
94 detection of antibodies from previous infections. In contrast, molecular diagnostic
95 techniques, including PCR and Loop-mediated isothermal amplification (LAMP), offer
96 increased sensitivity (73-100 %) and LoD (1-1000 parasites/mL) by targeting specific
97 regions of the parasites DNA. For the main AAT-related *Trypanosoma* species, pan-
98 species primers (targeting ITS1 for instance) and genus/species/type-specific primers
99 are available and currently used to detect the DNA of parasites from the subgenus
100 *Nannomonas* (*T. congolense*), *Duttonella* (*T. vivax*) and *Trypanozoon* (*T.b.brucei, T.*
101 *evansi* and *T. equiperdum*) (***Álvarez-Rodríguez et al., 2022; Desquesnes et al.,***
102 ***2022a***).

103 AAT-related trypanosome species circulate co-endemically with *T. b. gambiense* in
104 West and Central Africa, where domestic animals such as pigs, dogs, cattle, sheep
105 and goats are suspected reservoirs (***Magang et al., 2023; Traoré et al., 2021***). In
106 these regions, Suids (warthogs, domestic and bush pigs) and bovids (bushbucks and
107 buffalos) are the preferred hosts for most tsetse fly species (***Serem et al., 2024***). In a
108 historical HAT focus in Côte d'Ivoire, free-range pigs sharing the same environment as
109 humans were identified as reservoirs for *T. b. gambiense* (***Traoré et al., 2021***). The
110 diagnostic techniques employed in this study, involving single round (***Radwanska et***
111 ***al., 2002***) or nested PCR (***Morrison et al., 2008***), however tended to overestimate the
112 prevalence of the human infective parasites in pigs (***Traoré et al., 2021***). Therefore,
113 an active and accurate surveillance of the infection status of domestic animals using a
114 more reliable diagnostic tool will be key to reach and sustain gHAT elimination (***Simo***
115 ***and Rayaisse, 2015; Vourchakbé et al., 2020***). In addition, a comprehensive map of
116 the animal infective trypanosomes circulating in tsetse-infested areas would enable an
117 improved control strategy and prevent or limit further economic losses.

118 In this context, developing new diagnostic tools that are species-specific and highly
119 sensitive is essential to accurately diagnose infected individuals and define the
120 circulation of trypanosomes in domestic animals. For this purpose, we have adapted
121 the Specific High-sensitivity Enzymatic Reporter unLOCKing (SHERLOCK) detection
122 that offers unprecedented levels of diagnostic specificity and sensitivity (***Gootenberg***
123 ***et al., 2017***), and has been adapted for the detection of HAT (***Sima et al., 2022***).
124 SHERLOCK combines an isothermal amplification by recombinase polymerase (RPA)
125 with Cas13a detection of the target RNA (***Gootenberg et al., 2017; Kellner et al.,***

126 ***2019; Piepenburg et al., 2006***). The RPA step, in combination with a reverse
127 transcriptase, allows the use of total nucleic acid (TNA) as an input, increasing the
128 flexibility of the assay. Here, we have developed a broad panel of SHERLOCK assays
129 for the detection of the six most prevalent AAT-related species. We have applied the
130 SHERLOCK4AAT panel to two populations of domestic pigs from two eco-
131 epidemiological regions of West Africa to determine their importance as reservoirs of
132 both animal and human-infective trypanosomes. A total of 424 blood samples were
133 collected (1) from free-ranging pigs in the last hypo-endemic foci of gHAT in Côte
134 d'Ivoire, and (2) from farm pigs bred in the historical gHAT focus of forested Guinea
135 where unconfirmed seropositive cases of gHAT are still sporadically detected (***Courtin***
136 ***et al., 2019***). These samples were screened using the complete SHERLOCK4AAT
137 panel to provide an in-depth profile of the trypanosome species circulating among
138 these domestic animals.

139 **Materials and Methods**

140 Ethics statement

141 The only reliable method available to maintain and amplify field-isolated animal
142 trypanosomes is to experimentally infect laboratory animals, here mice. For this study,
143 experimental infections were carried out at UMR INTERTRYP and were approved by
144 the regional ethics committee for animal experimentation as part of the project APAFIS
145 #34149-2020091118136527v5 and authorized by the French Ministry for Higher
146 Education and Research. In Guinea, ethical approval was obtained from the *Comité*
147 *National d'Ethique pour la Recherche en Santé* (CNERS) under agreement number
148 102/CNERS/19. In Côte d'Ivoire, sample collection was conducted within the
149 framework of epidemiological surveillance activities supervised by the HAT National
150 Elimination Program (HAT-NEP). No ethical statement is required by local authorities
151 for domestic animal sampling. Any veterinarian may carry out blood sampling on
152 domestic animals, with the authorization of the owner, as it is performed during
153 prophylaxis or diagnostic campaign. Breeders gave their consent for animal sampling
154 after being informed of the objectives of the study. For pig care, venous sampling was
155 performed by a veterinary of the Laboratoire National d'Appui au Développement Rural
156 (Ministry of Agriculture).

157 Mice infection and parasite purification

158 24 hours prior to infection with trypanosome parasites, 8-week-old female BALB/c mice
159 (Charles River Laboratory) were immunosuppressed by intraperitoneal injection of 0.1
160 mL Endoxan 500 mg (Baxter). *T. congolense* Savannah subgroup IL1180 strain
161 (Tanzania, Serengeti 1971, STIB212), *T. vivax* Magnan strain (Burkina Faso, Magnan
162 2011) and *T. theileri* (Nederland, Utrecht 2003, UNUT) parasites (INTERTRYP unit's
163 cryobank) were inoculated by intraperitoneal injection of 0.15 mL of the cryopreserved
164 blood containing parasites. Two mice were infected per strain and parasitaemia was
165 monitored daily by tail blood sampling. Parasite yields were estimated by counting in a
166 fast read 102 counting cells (Kova). Whole blood was collected by cardiac puncture
167 under deep isoflurane anaesthesia when parasitaemia reached 1 x 10^8 cells per mL.
168 Infected blood was passed over a diethylaminoethyl (DEAE)-cellulose column and the
169 column washed using phosphate buffer saline (PBS) supplemented with 1 % glucose
170 (PBSG). Parasites were collected in PBSG and concentrated by centrifugation (2000
171 rpm, 10 min, RT).

172 Cell culture

173 *T. b. brucei* Lister 427 bloodstream form and *T. b. gambiense* ELIANE cells were
174 cultured in HMI-11 medium (ThermoFisher scientific) supplemented with 10 % fetal
175 bovine serum (Sigma) at 37°C with 5 % CO_2. Human embryonic kidney (HEK) 293T
176 cells were cultured in complemented dMEM (Merck) at 37°C with 5 % CO_2.

177 Epidemiological surveys

178 Pig blood samples were collected from the external jugular vein in heparinized tubes
179 during two independent surveys in Côte d'Ivoire and Guinea. In Côte d'Ivoire, 224 free-
180 ranging pigs were sampled in May, June and July 2021 in the Bonon and Sinfra
181 hypoendemic HAT foci, the Bouaflé and Vavoua historical HAT foci and the Brobo
182 HAT-free area {Kaba, 2023 #8655}. In Guinea, 200 farm pigs were sampled in March
183 2023 in the N'zérékoré prefecture, an ancient gHAT focus. Four drops of blood were
184 dried on 4th grade Whatman filter paper (Cytivia Life Sciences) and conserved in sealed
185 plastic bags with silica gel at ambient temperature for several months until total nucleic
186 acid (TNA) extraction.

187 Nucleic acid extraction

188 RNA was extracted from bloodstream form parasites (*T. b. brucei* Lister 427, *T. b.*
189 *gambiense* ELIANE, *T. congolense* Savannah subgroup IL1180, *T. vivax* Magnan and

190 *T. theileri*), HEK 293T cells and whole blood from French cattle, pig, sheep and goat
191 (Bergerie de la Combe aux Loups). Bloodstream form parasites from infected mice, as
192 well as cultured HEK 293T cells, were harvested in TRIzol (Life Technologies) and
193 Chloroform:Isoamyl alcohol (24:1, Sigma-Aldrich) was added, followed by
194 centrifugation at 13,000 rpm at 4°C for 15 min. The upper aqueous phase was
195 transferred to a fresh tube containing 0.5 mL of 75 % ethanol. After incubation for 10
196 min at room temperature, RNA was extracted using a NucleoSpin RNA column
197 (Macherey Nagel) or a RNAeasy kit (Qiagen) according to the manufacturer's
198 instructions. 500 µL of blood sampled from French cattle, pig, sheep and goats was
199 treated with 500 µL lysis buffer supplemented by 50 µL Proteinase K and incubated for
200 30 min at 56°C. The resulting mixture was transferred into a QIAshredder column
201 (Qiagen) and centrifuged at 13,000 rpm for 2 min. The flow-through was then used for
202 RNA extraction using a RNeasy Mini kit (Qiagen) according to the manufacturer
203 recommendations. After extraction, qualities and quantities of RNA were evaluated
204 using the NanoDrop™ One (Ozyme).

205 For extraction of TNA from dry blood spots (DBS), three 6 mm-punches from one spot
206 of each animal DBS were resuspended in 300 µL of lysis buffer supplemented by 30
207 µL of Proteinase K and incubated for 30 min at 56°C. The punches and liquid were
208 transferred into a QIAshredder column (Qiagen) and centrifuged at 13,000 rpm for 2
209 min. TNA was extracted from the flow-through using the Maxwell RSC Buccal Swab
210 Kit (AS1640) with the Maxwell RSC Instrument (AS4500) according to the
211 manufacturer's instructions. For each sample, all SHERLOCK assays were performed
212 from a single TNA extraction.

213 Target selection, RPA primers and crRNAs design

214 Alignments of the *18S rRNA*, *IFX* and *GAPDH* genes were performed on sequences
215 from different species (Supplementary Table 1) using Clustal Omega (***Sievers and***
216 ***Higgins, 2018***). The distance matrix representing the percentage identity between
217 each sequence was represented using GraphPad Prism software (V.10).

218 BLAST analysis (***McGinnis and Madden, 2004***) of the *18S rRNA* and *GAPDH* genes
219 selected target sequences was performed in the NCBI standard database of using the
220 following selection of organisms: Microsporidia (taxid:6029), Ciliophora (taxid:5878),
221 Haemosporida (taxid:5819), Diplomonadida (taxid:5738), Symbiontida (taxid:797087),
222 Diplonemea (taxid:191814), Euglenida (taxid:3035), Kinetoplastea (taxid:5653),

223 Metakinetosplastina (taxid:2704647), Trypanosomatida (taxid:2704949),
224 Trypanosomatidae (taxid:5654) and Euglenozoa (taxid:33682). The program selection
225 was optimized for somewhat similar sequences (blastn) and in algorithm parameters,
226 the maximum number of aligned sequences to display was set as 5000.

227 The presence of single nucleotide polymorphism (SNPs) in the target regions was
228 assessed by aligning sequence variants of the parasite species using Clustal Omega
229 (***Sievers and Higgins, 2018***). Sequence variants used are listed in Supplementary
230 Table 1. SNPs identified in the TriTrypDB (https://tritrypdb.org) database were also
231 taken into account in the design: NGS_SNP.Tb927_03: v5.1.921431, v5.1.921465,
232 v5.1.921571, v5.1.921612, v5.1.921937, v5.1.922234, v5.1.922298, v5.1.922511,
233 v5.1.922637, v5.1.922803, v5.1.923180, v5.1.959274; NGS_SNP.Tb927_07:
234 v5.1.1951525, v5.1.1952283, v5.1.1951291; NGS_SNP.Tb927_02: v5.1.371291,
235 v5.1.371584 and v5.1.370058.

236 Primers for Recombinase Polymerase Amplification (RPA) of targeted regions were
237 designed in Primer-BLAST (***Ye et al., 2012***) using the customised parameters
238 described by (***Kellner et al., 2019***). Oligonucleotides prone to generate self-dimers or
239 cross primer dimers detected by Multiple Primer Analyzer (ThermoFisher) were
240 discarded. Primers selected for each SHERLOCK assays are listed and highlighted in
241 Supplementary Table 2. The T7 promoter sequence (5'
242 GAAATTAATACGACTCACTATAGGG) was added at each 5' end of the selected
243 forward primers to enable the *in vitro* transcription necessary for Cas13a detection
244 (***Kellner et al., 2019***).

245 <u>Production of crRNAs and positive controls</u>

246 crRNA production was carried out as previously described (***Kellner et al., 2019; Sima***
247 ***et al., 2022***). Briefly, each crRNA DNA template, containing the spacer (specific
248 targeted region) followed by the direct repeat (5'
249 GATTTAGACTACCCCAAAAACGAAGGGGACTAAAAC) and the T7 promoter
250 sequence, were *in vitro* transcribed using the HiScribe™ T7 Quick High Yield RNA
251 Synthesis Kit (NEB) and purified using magnetic beads (Agencourt RNAClean XP).
252 DNA template sequences used for the synthesis of each crRNA are detailed in
253 Supplementary Table 2.

254 For the production of the synthetic positive controls, *in vitro* transcription of the targets
255 was performed as previously described (***Sima et al., 2022***) using RNA from the target
256 species for each specific assay. The amount of template used to produce the positive
257 control for each assay were as follows: 200 ng of RNA from *T. b. brucei* Lister 427 for
258 18S pan-trypanosomatid and 18S pan-*Trypanozoon* assays, 120 ng of RNA from *T. b.*
259 *gambiense* ELIANE strain for TgSGP assay, 120 ng of RNA from *T. vivax* Magnan
260 strain for IFX assay, 230 ng of RNA from *T. congolense* Savannah subgroup IL1180
261 strain for 18S *T. congolense*-specific assay and 5 ng of RNA from *T. theileri* for 18S *T.*
262 *theileri*-specific assay. Due to a lack of *T. simiae* and *T. suis* genetic material, the
263 positive controls were synthesized at Eurogentec using the *in-silico* predicted
264 sequence of the target region. Primers and target regions used to produce positive
265 controls are listed in the Supplementary Table 3.

266 SHERLOCK assays

267 SHERLOCK assays were performed as previously described (***Kellner et al., 2019;***
268 ***Sima et al., 2022***). RPA was performed using the TwistAmp Basic kit (TwistDx)
269 following manufacturer's instructions with slight modifications. To enable reverse
270 transcription of the RPA (RT-RPA), 2.2 U of transcriptor reverse transcriptase (Roche)
271 were added to the reaction. Specific RPA primer pairs were used for each target
272 amplification at a concentration of 480 nM per primer, and the amplification reaction
273 was carried out in a heating block at 42°C for 45 minutes (***Sima et al., 2022***).
274 *Leptotrichia wadeii* Cas13a (*Lw*Cas13a) enzyme was produced as previously
275 described (***Kellner et al., 2019; Sima et al., 2022***). Briefly, pC013-Twinstrep-SUMO-
276 huLwCas13a plasmid (Addgene plasmid #90097) was inserted into *Escherichia coli*
277 RosettaTM 2(DE3) pLysS competent cells for *Lw*Cas13a expression and purification
278 (Gootenberg et al. 2017). Purified *Lw*Cas13a was conserved in Storage buffer (SB:
279 Tris-HCl 1M, NaCl 5M, DTT 1M and glycerol) (***Kellner et al., 2019***) in single-use
280 aliquots at -80°C to avoid freeze-thaw cycles.

281 The Cas13a-crRNA mediated target detection reaction was performed simultaneously
282 with the *in vitro* transcription of the target amplified by RT-RPA. *In vitro* transcription of
283 the amplified target was performed using T7 RNA polymerase (Biosearch technology).
284 Each Cas13a detection reaction was run in triplicate on a TECAN plate reader
285 (INFINITE F200 PRO M PLEX) and fluorescence readouts were collected every 10
286 minutes for 3 hours. All reactions were carried out with the inclusion of a negative

287 control template (NCT) adding nuclease-free water as input, and a positive control
288 template (PCT), here the *in vitro* produced positive control for each specific
289 SHERLOCK. For screening samples from epidemiological surveys, the same protocol
290 as described above was used, except a TECAN plate reader (INFINITE F200 PRO
291 Option Infinite F Nano +) was used and the assay was performed without replicates.
292 Optimizations were carried out either at Institut Pasteur in Paris (France) or at
293 INTERTRYP unit in Montpellier (France), while analysis of samples from
294 epidemiological surveys was carried out at Institut Pasteur of Guinea.

295 Data representation and statistical analyses

296 Fold-change over background fluorescence was used to represent fluorescence
297 readouts for all SHERLOCK assays. Background fluorescence is given by the NCT
298 evaluation, where water is used as input material for the RPA reaction. For each test,
299 sample fluorescence obtained after 3 hours of reading was divided by NCT
300 fluorescence at the same time.

301 $$FC = \frac{Fsample\ t = 3h}{Fnct\ mean\ t = 3h}$$

302 Where *FC* represents Fold-Change over background fluorescence, *Fsample t=3h*
303 represents sample fluorescence obtained after 3 hours and *Fnct mean t=3h* represents
304 NCT fluorescence after 3 hours of reactions.

305 Analytical characteristics including threshold, sensitivity and specificity of each
306 SHERLOCK assay were evaluated using Receiver Operating Characteristic (ROC)
307 curves calculation comparing NCT versus PCT at controlled dilutions of parasites or
308 hosts genetic materials. Results obtained from SHERLOCK specific assays on
309 targeted parasites were gathered in a positive sample column, while results obtained
310 from NCT, hosts and non-targeted parasites analysed with the assay, were placed in
311 a negative sample column for ROC curve calculation and threshold evaluation. ROC
312 curves were calculated using the Wilson/Brown method with a 95 % confidence interval
313 and threshold values were selected based on the Youden's index (sensitivity +
314 specificity – 1), that defines an optimal threshold as the one that maximizes the index
315 of classification accuracy (***Brown et al., 2001; Schisterman et al., 2005***). The
316 threshold of positivity for each SHERLOCK assay was selected from ROC analyses
317 as the value corresponding to the maximum specificity (100 %). The limit of detection

318 (LoD) of each SHERLOCK reaction was assessed using specific tests on serial
319 dilutions of target parasite RNA. Dilutions ranged from 5.10^3 pg/µL (equivalent to 10^7
320 parasites/mL) to 5.10^{-5} pg/µL (equivalent to 0.1 parasites/mL). All plots and statistical
321 analyses were performed with GraphPad Prism software (V.10). The Venn diagrams
322 were made based on the Venny model by Oliveros J.C. (BioinfoGP, CNB-CSIC).

323 Maps were generated with the QGIS software version 3.42.0 with backgrounds
324 retrieved from data.gouv.fr (OSM2IGEO - Ivory Coast - SHP - EPSG:4326 for Côte
325 d'Ivoire, and OSM2IGEO - Guinea - SHP - EPSG:4326 for Guinea).

326 In the absence of reliable infection status in the field data from pigs, the posterior
327 distributions of performance estimates, such as sensitivity (Se), were jointly estimated
328 with a Bayesian latent class model (***Joseph et al., 1995***). The model takes boolean
329 outcomes (either positive or negative) of several tests as input. This Monte Carlo
330 method operates based on a Gibbs sampling process. The model iteratively updates
331 both the test performance parameters (sensitivity, specificity, and frequency of positive
332 individuals in sample collection) and the latent infection status. Flat prior was used.
333 After visually controlling that stationarity of the chain was quickly reached, we
334 discarded the first 150 burn-in iterations and calculated posterior densities based on >
335 10,000 iterations. 95 % confidence intervals were calculated for each proportion to
336 quantify the uncertainty of the estimates, providing a scientific range within which the
337 population proportions are likely to be accurate (***Brown et al., 2001***).

338 **Results**

339 <u>Selection of targets for broad and species-specific SHERLOCK assays targeting AAT</u>
340 <u>species (SHERLOCK4AAT).</u>

341 Target gene selection was based on two requirements: to develop (a) a broad
342 SHERLOCK assay for the detection of all trypanosomatid parasites and (b) for species
343 discrimination. To adapt SHERLOCK for the detection of AAT-related species, we
344 followed the criteria as described in (***Sima et al., 2022***). Briefly, candidate genes must
345 (1) be expressed in the bloodstream form of the parasites, (2) be conserved between
346 strains, (3) have few or no single nucleotide polymorphisms (SNPs), or (4) show
347 sequence divergence that would allow for species discrimination. All RPA primers and
348 crRNAs designed for each SHERLOCK assays are listed in Supplementary Table 2.

349 **Pan-trypanosomatid assay.** SHERLOCK has the capacity to discriminate between
350 two sequences differing by a single nucleotide (***Gootenberg et al., 2017***). This study
351 therefore focused on regions of the *18S rRNA* gene that show limited sequence
352 homology between species. In addition to being a multicopy gene, the *18S rRNA* gene
353 shares over 70 % identity between Kinetoplastea members (Supplementary Figure 1).
354 Using BLAST analysis, the region between 1535-1672 bp (XR_002989632.1) was
355 found to be conserved between all trypanosomatid species and was selected as the
356 pan-trypanosomatid SHERLOCK target. RPA primers were designed to amplify this
357 138 bp region using Primer-Blast (***Ye et al., 2012***) (Supplementary Figure 2A and
358 Supplementary Table 2). The level of identity of the target region was assessed
359 between the different sequences described in the Trypanosomatidae family, as well as
360 in the order, subclass and class that contain this family (Supplementary Figure 3).
361 Examination of the Euglenozoa phylum, excluding the Kinetoplastea class, showed
362 98.4 % identity within the Trypanosomatidae family and 97.3 % identity within the
363 Kinetoplastea class (Supplementary Figure 3). This was reduced to 82.9 % for the
364 Phylum Euglenozoa, excluding the Kinetoplastea sequences (Supplementary Figure
365 3). Three distinct crRNAs were designed to this region, which can be used individually
366 or multiplexed to increase the sensitivity (Supplementary Figure 4A and
367 Supplementary Table 2). The sequences described in each group were 100 %
368 conserved to the crRNA. RPA primers and crRNA targets of the pan-trypanosomatid
369 SHERLOCK assay target regions (Kinetoplastea) were then compared to the
370 homologous sequences from other classes within the Phylum Euglenozoa (Euglenida,
371 Diplonemea, Symbiontida and Kinetoplastea) (Supplementary Figure 2A and 3). In
372 addition, sequences from related protozoan parasite classes (Diplomonadida,
373 Haemosporida and Ciliophora) and from the genetically close but phylogenetically
374 distinct group Microsporidia were also included in the analysis (Supplementary Figure
375 2A).

376 **Pan-*Trypanozoon* assay**. A pan-*Trypanozoon* SHERLOCK assay was designed for
377 increased selectivity to especially detect *T. brucei s.l.* (*sensu lato*). The regions within
378 the 18S rRNA that were highly conserved among the species of the *Trypanozoon*
379 subgenus, while showing significant divergence from other trypanosome species not
380 belonging to the *Trypanozoon* subgenus, were analysed (Supplementary Figure 2B).
381 A region ranging from 1318 to 1433 bp (XR_002989632.1) (Figure 1A and

382 Supplementary Table 2) was selected as it showed high conservation among the
383 *Trypanozoon* subgenus (99.12 - 100 % percentage of identity, query coverage >90 %),
384 except for three *T. evansi* sequences (91.96 - 96.49 %, OL869590.1, KT844944.1,
385 MF142286.1). The crRNA target region selected was also conserved in the subgenus
386 *Trypanozoon* and divergent in other parasites. Specific alignments with trypanosome
387 species that could share the same hosts (*T. congolense*, *T. vivax*, *Leishmania spp.*,
388 etc) were performed to assess target amplicon specificity (Supplementary Figure 2B).
389 The pan-*Trypanozoon* SHERLOCK assay can discriminate between the species
390 belonging to the *Trypanozoon* subgenus (*T. b. spp., T. evansi* types A and B, and *T.*
391 *equiperdum*) from other non-*Trypanozoon* trypanosomes or other co-endemic
392 parasites.

393 **Species-specific assays**. For species discrimination within a single sample, several
394 SHERLOCK assays were developed to detect the most prevalent species causing
395 AAT. These include *T. congolense*, *T. vivax*, *T. theileri*, *T. simiae* and *T. suis*.

396 *T. congolense*: Regions conserved in the *18S rRNA* gene for all described *T.*
397 *congolense* sequences, including the Savannah, Forest, Kilifi and Dzanga-Sangha
398 groups, were analysed. The target region selected from position 116 to 246 bp of the
399 *18S rRNA* gene (AJ009146.1) shows 100 % identity between the described *T.*
400 *congolense* sequences. BLAST analysis of the *T. congolense 18S rRNA* gene
401 sequences, excluding the target species (*T. congolense*, (taxid: 5692)) was also
402 performed to determine the percentage of identity of closely related species. *T. simiae*
403 (86.72 to 90.62 %), *T. sapaensis* (88.28 %), *T. godfreyi* (88.28 %), and *T.*
404 *otospermophili* (87.02 %) had the highest percentage identity observed
405 (Supplementary Figure 5). Species with common hosts and of veterinary relevance
406 such as the two analysed *T. vivax* strains showed 82.81% and 87.5% identity. In
407 addition, none of these sequences were fully conserved for the selected crRNA
408 (Supplementary Figure 5), ensuring the specificity of the test and the absence of cross-
409 detection with other species.

410 *T. vivax*: The *invariant flagellum antigen* (*IFX*) gene has no apparent homologue in any
411 other *Trypanosoma* species or other related parasites, and was therefore selected
412 (***Autheman et al., 2021; Romero-Ramirez et al., 2022***). BLAST analysis, using *T.*
413 *vivax* Y486 (HE573024.1) as a reference genome, resulted in no matches (Figure 1A
414 and Supplementary Table 2).

415 *T. theileri*: A conserved region between the three *T. theileri* lineages (TthI, TthII and
416 TthIII) (***Brotánková et al., 2022***) was selected. The target region, ranging from 1014
417 to 1158 bp of the *18S rRNA* gene (AJ009163.1), has 100 % identity between the
418 described sequences of the *T. theileri* lineages, and the most closely related
419 sequences were from *T. cruzi*, *T. rangeli* and *T. dionisii*, with a 97.89 % identity (query
420 coverage =65 %). The segment 1052-1081 bp corresponding to the crRNA sequence,
421 is highly conserved between *T. theileri* variants (Figure 1A and Supplementary Table
422 2), however it contains a SNP (1060 C/T) in a number of the sequences analysed.
423 Hence, one RPA primer pair and two multiplexed crRNAs were designed to target both
424 version of the SNP for the *T. theileri* SHERLOCK assay (Supplementary Figure 4E).

425 *T. simiae:* The region from 1246-1346 bp of the *18S rRNA* gene (AJ404608.1) was
426 selected as the targeted region for RPA amplification of the *T. simiae*-specific
427 SHERLOCK assay. The segment 1273-1299 bp that corresponds to the crRNA
428 sequence, has 100 % identity between the described sequences of *T. simiae* (Figure
429 1A and Supplementary Table 2).

430 *T. suis:* The multicopy *GAPDH* gene was used, as it can be phylogenetically separated
431 into *T. suis* and *T. suis*-like strains from other African trypanosomes (***Rodrigues et al.,***
432 ***2020***). The region from 389 to 528 bp of the *GAPDH* gene (MK962702.1) has been
433 selected as the targeted region for RPA amplification of the *T. suis*-specific
434 SHERLOCK assay (Figure 1A and Supplementary Table 2). This region is 100 %
435 conserved between the *T. suis* species described, and outside this clade, the most
436 closely related sequences were found in *T. congolense*, with a 90 % of identity (query
437 coverage >90 %). The segment 410-437 bp of the *gGAPDH* gene (MK962702.1), that
438 corresponds to the crRNA target region, is highly conserved between *T. suis* species,
439 with 100 % identity, and the BLAST analysis showed that this target fragment can only
440 align to *T. suis* sequences but not to that of other Kinetoplastea species (taxid:5653).

441 <u>SHERLOCK can discriminate between closely related AAT-causing trypanosomatid</u>
442 <u>species.</u>
443 All RPA primers and crRNAs for each targeted species were screened to select the
444 optimal combinations, with the highest specificity and selectivity. For the pan-
445 trypanosomatid assay, RPA primer pair A was used to screen three crRNAs
446 (A:crRNA1, A:crRNA2 and A:crRNA3; Supplementary Figure 4A). From this, crRNA 3
447 was first selected for the simple pan-trypanosomatid assay. For the pan-*Trypanozoon*

448 assay, three RPA primer pairs (A, B and C) were screened with two crRNA candidates
449 each (A:crRNA1, A:crRNA2, B:crRNA1, B:crRNA2, C:crRNA1, C:crRNA2,
450 Supplementary Figure 4B). The A:crRNA1 combination was selected for the pan-
451 *Trypanozoon* assay, being the one that obtained a higher fold change for the positive
452 control and a lower fold change for the negative control. For the IFX *T. vivax* species-
453 specific SHERLOCK assay, two RPA primer pairs were assessed (A and B) in
454 combination with six crRNA candidates (A:crRNA1, A:crRNA2, A:crRNA3, B:crRNA4,
455 B:crRNA5, B:crRNA6). RPA primer pair B and crRNA 6 showed the lowest variability
456 between replicates and without any cross-reaction with other trypanosome species
457 (Supplementary Figure 4C). For the *T. congolense*-specific assay, one pair of RPA
458 primer (A) was combined with ten crRNA candidates (A:crRNA1, A:crRNA2,
459 A:crRNA3, A:crRNA4, A:crRNA5, A:crRNA6, A:crRNA7, A:crRNA8, A:crRNA9,
460 A:crRNA10). The crRNA1 that exhibited the lowest inter-replicate deviation and no
461 cross-reactivity when exposed to the genetic material of non-target trypanosomatid
462 parasites was selected (Supplementary Figure 4D). For the *T. theileri*-specific
463 SHERLOCK assay, the combination of the RPA primer pair A with the two designed
464 crRNAs (1 and 2) was used to cover the specific detection of all the *T. theileri* described
465 sequences (Supplementary Figure 4E). For *T. simiae* and *T. suis*, single combinations
466 of RPA primer and crRNA were tested. The specificity of each of these combinations
467 was also verified by comparing the specific recognition of each RNA target to RNA
468 from human embryonic kidney cell (HEK) (for pan-trypanosomatid and pan-
469 *Trypanozoon* tests) or RNA from *T. brucei* (for *T. vivax*, *T. congolense* and *T. theileri*
470 tests) (Supplementary Figure 4). In total, one RPA primer-crRNA combination was
471 selected for each assay, based on the highest fold change over background
472 fluorescence value, the highest specificity, and the minimum standard deviation
473 (Figure 1A).

474 The specificity of the RPA primer-crRNA combinations selected for each assay was
475 then cross-assessed against closely related parasites (Figure 1B-C). The single pan-
476 trypanosomatid assay detected RNA from all trypanosomatid species tested (*T. b.*
477 *brucei*, *T. b. gambiense*, *T. b. rhodesiense*, *T. evansi* (type A and B), *T. equiperdum*,
478 *T. congolense*, *T. vivax*, *T. theileri*, *T. cruzi* and *Leishmania major*) but not from HEK
479 cells, synthetic controls for *T. simiae* and *T. suis* or co-endemic parasites such as
480 *Plasmodium falciparum* (Figure 1B). The pan-*Trypanozoon* assay detected only RNA

481 from members of the *Trypanozoon* subgenus (*T. b. brucei*, *T. b. gambiense*, *T. b.*
482 *rhodesiense*, *T. evansi* (type A and B) and *T. equiperdum*) but not from HEK cells,
483 synthetic controls for *T. simiae* and *T. suis* or co-endemic parasites such as *T.*
484 *congolense*, *T. vivax*, *T. theileri* and *Plasmodium falciparum* (Figure 1B). The species-
485 specific *T. congolense*, *T. vivax*, *T. theileri*, *T. simiae* and *T. suis* assays only detected
486 their respective targeted parasite RNA or synthetic controls with no cross reactivity with
487 any other RNAs (Figure 1C). Additionally, no unspecific cross-reaction was observed
488 with the host-derived genetic material, as assessed by testing RNA from pig blood
489 (SHERLOCK single pan-trypanosomatid and pan-*Trypanozoon* assays in
490 Supplementary Figure 7).

491 The analytical sensitivity of each assay was quantified using serial dilutions of positive
492 control RNAs from known numbers of parasites. For the single pan-trypanosomatid
493 assay, the LoD was between 10 to 10^3 parasites per mL. The pan-*Trypanozoon* and
494 *T. theileri* assays tested 10 parasites per mL. For the *T. congolense* assay, the LoD
495 was found between 10 and 10^3 parasites per mL, and between 10^4 and 10^5 parasites
496 per mL for the *T. vivax* test (Figure 2A). The sensitivity of *T. simiae* and *T. suis* tests
497 were evaluated on synthetic positive controls, as no genetic materials were available,
498 and both showed a LoD between 10 and 100 fM (Figure 2B).

499 Then, to improve the sensitivity of the simple pan-trypanosomatid assay, crRNA1 was
500 tested in combination with crRNA3 for target recognition, as both crRNAs fall within the
501 same RPA amplicon A (Figure 3A). Comparative analyses between the two versions
502 were performed and multiplexing was shown to increase the performance of the assay,
503 especially for the lower dilutions evaluated (100, 500 and 10^3 p/mL) by increasing the
504 fold-change readouts of these positive controls by 1, 2.5 and 3-fold-change units,
505 respectively (Supplementary Figure 6). Using results obtained on the blood samples
506 from pigs in Côte d'Ivoire (see next section), we compared the two versions of the pan-
507 trypanosomatid SHERLOCK assays to determine the posterior distribution of
508 sensitivity estimates. We applied a Monte Carlo method (Gibbs sampling) proceeding
509 in an iterative chain using the infection frequency, specificity, and sensitivity of the two
510 tests to update the infection status. We determined the posterior sensitivity distribution
511 of the simple versus multiplex pan-trypanosomatid SHERLOCK assays. Multiplexing
512 crRNAs increased the median sensitivity from 66.1 % to 74.7 %, while keeping
513 specificity above 80 % (Figure 3B). Furthermore, a higher concordance was observed

514 between the results obtained on the same samples with the pan-*Trypanozoon*
515 SHERLOCK assay and the multiplexed pan-trypanosomatid SHERLOCK assay
516 (25.7-% of double positives), as compared to the simple version (7.8 % of double
517 positives) (Figure 3C). Given its improved detection efficiency, the multiplex version of
518 the 18S rRNA pan-trypanosomatid assay was subsequently used exclusively and
519 referred to as the multiplex pan-trypanosomatid assay.

520 To determine a positivity threshold value (fold-change cut-off) for each SHERLOCK
521 assay, ROC curve analyses were performed and use to evaluate each following
522 analytical sensitivity and specificity. The positivity threshold values were 6.050 for the
523 pan-trypanosomatid test, 11.70 for the pan-*Trypanozoon* test, 1.923 for the *T.*
524 *congolense* test, 1.831 for the *T. vivax* test, 1.805 for the *T. theileri* test, 1.546 for the
525 *T. simiae* test, and 2.609 for the *T. suis* test (Supplementary Figure 8). Subsequently,
526 for a given test, any sample with a fold change value above the threshold was
527 considered positive for this test. Unsurprisingly, assays designed against multiple copy
528 genes (*18S rRNA* and *GAPDH*) showed a greater sensitivity than those targeting single
529 copy genes (*IFX*). Taken together, all the validated tests were able to specifically detect
530 the RNA targets for which they were designed, making it possible to distinguish
531 between closely related trypanosomatid parasite species. We then applied this novel
532 SHERLOCK4AAT toolbox was applied to the analysis of field samples in a molecular
533 eco-epidemiological survey.

534 <u>Application of the SHERLOCK4AAT toolbox to eco-epidemiological surveys in pigs.</u>
535 In transmission foci of western Africa, domestic pigs can host multiple trypanosome
536 species. To investigate this, the SHERLOCK4AAT toolbox was used to survey
537 trypanosomes circulating in domestic pigs from hypo-endemic and historical foci in
538 Côte d'Ivoire and Guinea. In Côte d'Ivoire, blood samples were collected from 224 free-
539 ranging pigs across the rural districts of Bonon, Bouaflé, Sinfra, Vavoua, and Brobo
540 (Figure 4A). In the N'zérékoré prefecture of Forested Guinea, 200 farm pigs were
541 sampled, with a focus on organized farming communities (Figure 5A). In addition to
542 the SHERLOCK4AAT toolbox assays, all samples were also screened for *T. b.*
543 *gambiense* using the previously described TgsGP SHERLOCK assay (***Sima et al.,***
544 ***2022***).

545 In total, 74.6 % [68.9, 80.3] (167/224) of the samples tested positive in at least one
546 SHERLOCK assay in Côte d'Ivoire (Figure 4B), and 49.5 % [42.6, 56.9] (99/200) in

547 Guinea (Figure 5B) representing a high apparent prevalence of trypanosome infections
548 in these two populations of pigs. In parallel, 47.3 % [40.8, 53.8] (106/224) of the pigs
549 from Côte d'Ivoire tested positive using at least one parasitological method (buffy coat
550 examination, mAECT and /or isolation in mice; results detailed in a separate study,
551 manuscript in preparation). No systematic parasitological data was available for
552 Guinean samples. The difference in positivity rates between SHERLOCK detection
553 and parasitological approaches on Ivoirian samples was likely due to the higher
554 sensitivity of SHERLOCK as compared to classical methods. Indeed, we compared
555 three SHERLOCK assays (multiplex pan-trypanosomatid, pan-*Trypanozoon* and *T.*
556 *congolense*-specific SHERLOCK assays) to the three parasitological tests (buffy coat
557 examination, mAECT and /or isolation in mice) to determine the posterior distribution
558 of sensitivity estimates. A Monte Carlo method (Gibbs sampling) was used by
559 proceeding in an iterative chain using the infection frequency, specificity, and
560 sensitivity of the tests to update the infection status. This analysis suggested that, in
561 terms of sensitivity, the combination of SHERLOCK4AAT assays may compete with
562 combined parasitological methods (i.e., median sensitivity 91.4 % vs 84.3 %) while
563 controlling median specificity above 75 % (Supplementary Figure 9). Importantly, in
564 contrast to parasitological tests, SHERLOCK4AAT allowed for the identification of the
565 trypanosome species involved in more than half of these infections.

566 Using the multiplex pan-trypanosomatid assay, 41.1 % [34.6, 47.6] of the samples from
567 Côte d'Ivoire (90/219) and 29.5 % [23.2, 35.8] from Guinea (59/200) were positive
568 (Figure 4C and 5C). The pan-*Trypanozoon* assay identified 38.0 % [31.6, 44.4]
569 (85/224) and 39.0 % [32.2, 45.8] (78/200) of samples in each country respectively
570 (Figure 4C and 5C). As there is no specific test for *T. b. brucei*, samples that were
571 positive in the pan-*Trypanozoon* assay but negative in the TgsGP assay were
572 presumed to be *T. b. brucei* infections. Only one sample tested positive in the *T. b.*
573 *gambiense*-specific assay in each country (Figure 4B and 5B). The TgsGP-positive
574 sample from the district of Bonon, Côte d'Ivoire was negative for all other SHERLOCK
575 assays, as well as in all parasitological tests. In contrast, the TgsGP-positive sample
576 from Guinea was positive in the multiplex pan-trypanosomatid SHERLOCK assay, as
577 well as in the CATT and mAECT tests, but it was negative in the pan-*Trypanozoon*
578 SHERLOCK assay. To further explore trypanosome diversity, species-specific
579 SHERLOCK assays for AAT were applied to the samples. In total, 23.2 % [17.7, 28.7]

580 (52/224) of the samples in Côte d'Ivoire and 7.5 % [3.8, 11.2] (15/200) in Guinea were
581 positive for *T. congolense*. Additionally, a single sample from Côte d'Ivoire tested
582 positive in the *T. suis*-specific SHERLOCK assay. Furthermore, no RNA from *T. vivax*
583 or *T. theileri* was detected with the IFX SHERLOCK assay.

584 Interestingly, a substantial number of co-infections were observed. In total, 24/219
585 individuals (11.0 ± 4.1 %) in Côte d'Ivoire and 13/200 in Guinea (6.5 ± 3.4 %) tested
586 positive in the multiplex pan-trypanosomatid, the pan-*Trypanozoon* and the *T.*
587 *congolense*-specific assays. These triple positive results indicate co-infections
588 involving both a *Trypanozoon* species (likely *T. b. brucei*) and *T. congolense* (Figure
589 4D and 5D). In addition, 9/219 samples (4.1 ± 2.6 %) from Côte d'Ivoire tested positive
590 in the pan-*Trypanozoon* and the *T. congolense* assays, which also represented co-
591 infections with *T. brucei s.l.* and *T. congolense*. Overall, 15.2 % [10.5, 19.9] of the
592 samples from Côte d'Ivoire showed co-infections with a *Trypanozoon* species and *T.*
593 *congolense*. Additionally, 15 samples from Côte d'Ivoire tested positive in both the
594 multiplex pan-trypanosomatid assay and the *T. congolense*-specific assay or were
595 positive only for *T. congolense*. In Guinea, two samples tested positive in both the *T.*
596 *congolense*-specific and multiplex pan-trypanosomatid SHERLOCK assays,
597 indicating *T. congolense* mono-infections (Figure 4D and 5D).

598 Furthermore, 56 samples (25.6 ± 5.8 %) in Côte d'Ivoire, and 38 samples (19.0 ± 5.4
599 %) in Guinea tested positive in both the multiplex pan-trypanosomatid and the pan-
600 *Trypanozoon* SHERLOCK assays. In contrast, 17 samples from Côte d'Ivoire and 40
601 from Guinea tested positive in the pan-*Trypanozoon* assay but negative in the multiplex
602 pan-trypanosomatid assay, likely due to the lower sensitivity of the latter. Lastly, 19
603 samples (8.7 ± 3.7 %) in Côte d'Ivoire and 19 samples (9.5 ± 4.1 %) in Guinea tested
604 positive in the multiplex pan-trypanosomatid assay only (Figure 4D and 5D). The
605 absence of positivity in the *T. congolense*, *T. simiae* and *T. suis*-specific assays may
606 be due to their lower sensitivity, or to infections with other non-targeted trypanosome
607 species.

608 **Discussion**

609 The SHERLOCK4AAT toolbox, a new panel of highly sensitive and specific high-
610 throughput assays for detecting animal trypanosomes.

611 Species identification is essential for assessing both the distribution of prominent
612 parasites impacting veterinary health and spotting reservoirs for human-infective
613 trypanosomes. In a context where symptoms are often mild and unspecific, especially
614 in hosts like pigs, accurate species-specific detection methods are essential. Ideally,
615 diagnostic assays should be able to analyse both fresh and stored (ambient
616 temperature) samples to determine parasites circulating within a specific area.

617 In this study, conserved and species-specific targets have been used to adapt
618 SHERLOCK for the detection of most members of the Trypanosomatidae family
619 (Kinetoplastea class) (Supplementary Figure 3) of veterinary importance (pan-
620 trypanosomatid), and species-specific assays to discriminate between the six most
621 common animal trypanosomes species in the study regions: *Trypanozoon* (*T. b. brucei*,
622 *T. evansi* and *T. equiperdum*), *T. congolense* (Savanah, Forest Kilifi and Dzanga-
623 sangha), *T. vivax*, *T. theileri* (TthI, TthII and TthIII), *T. simiae* and *T. suis*. The design
624 of both broad and species-specific assays was based primarily on sequences of the
625 *18S rRNA* and *GAPDH* genes which, as well as being conserved across species
626 (Supplementary Figure 1), are highly expressed and contain regions that allowed for
627 species discrimination. However, for *T. vivax*, the single-copy *IFX* gene was selected
628 for its high specificity (***Romero-Ramirez et al., 2022***). The first simple version of our
629 pan-trypanosomatid assay employed a single crRNA guide and was previously used
630 to evaluated blood samples from gHAT seropositive individuals with a specificity of 93
631 % (95.4-98.6) (***N'Djetchi et al., 2024***). To increase the performances of this assay, we
632 added a second crRNA guide into the reaction mix to target the same RPA amplicon
633 during the SHERLOCK reaction, resulting in an increased test sensitivity (Figure 3 and
634 Supplementary Figure 6). For *Trypanozoon* species, no sequences were identified to
635 distinguish *T. b. brucei*, *T. evansi* (A and B) and *T. equiperdum* as these parasites
636 cannot be easily differentiated using the *18S rRNA* gene. In the future, other genes
637 such as *RoTat1.2 VSG* or *ESAG6/7* could be explored to discriminate *T. evansi* from
638 other *Trypanozoon* by SHERLOCK (***Claes et al., 2004; Holland et al., 2001***). Overall,
639 *in silico* and *in vitro* analyses enabled us to assess the analytical specificities of these

640 new SHERLOCK assays, confirming that the targets selected were sufficiently specific
641 to be used as diagnostic for the species and groups of species concerned.

642 Using parasite RNAs, the LoD of the SHERLOCK assays were estimated to range
643 between 10 to 10^3 parasites/mL for the pan-trypanosomatid assay, 10 parasites/mL for
644 the pan-*Trypanozoon* and *T. theileri* assays, from 10 to 10^3 parasites/mL for *T.*
645 *congolense* and 10^4-10^5 parasites/mL for *T. vivax*. Most PCR-derived molecular
646 techniques currently used for detecting animal trypanosomes have a detection limit of
647 1 to 10 parasites/mL using genus- or species-specific primers, 50 parasites/mL using
648 pan-species ITS1 primers (***Desquesnes et al., 2022a***) or 5 parasites/mL using 18S
649 rRNA-targeting primers (***Deborggraeve et al., 2006***). The ROC analyses of the *T.*
650 *brucei*, *T. congolense* and *T. vivax* SHERLOCK assays (Supplementary Figure 8C)
651 also shown sensitivity and specificity comparable to those of the recently developed
652 7SL sRNA diagnostic test for Animal trypanosomosis (***Contreras Garcia et al., 2022***).
653 Therefore, in total, the analytical sensitivities obtained by the pan-trypanosomatid, pan-
654 *Trypanozoon*, *T. theileri* and *T. congolense* SHERLOCK assays were comparable with
655 those of other existing molecular tools. Yet, a significant difference in favour of using
656 SHERLOCK4AAT is that it detects RNAs, probing for active infections. The *T. vivax*
657 SHERLOCK assay, targeting the single-copy *IFX* gene (***Autheman et al., 2021***), did
658 not meet the sensitivity requirements for the molecular diagnosis of animal
659 trypanosomes and would require the identification of another target. As no genetic
660 material from parasites was available for developing *T. simiae* and *T. suis* SHERLOCK
661 assays, LoDs were determined using synthetic RNA controls. Both assays were able
662 to detect 10 to 100 fM of the synthetic controls, far from the detection capacity of
663 SHERLOCK, which can detect synthetic targets at a concentration of 2 aM in optimal
664 conditions (***Gootenberg et al., 2017***).

665 In the current version of the SHERLOCK4AAT toolbox, each assay can be run in 2 h
666 30 min, in a two-step reaction, at 2.5 € (exclusive of initial sample processing) (***Sima***
667 ***et al., 2022***). All tests are optimized for high throughput screening with a fluorescence
668 readout; hence, they can be performed in standard lab conditions by a technician
669 trained for basic molecular biology. SHERLOCK4AAT was not developed for direct
670 case diagnosis in the field, but rather for eco-epidemiological surveillance at large
671 scale. Considering the absence of trypanosome species-specific treatment for
672 domestic animals, the future development of a RDT for AAT would only include the

673 pan-trypanosomatid target or equivalent. This would however require further technical
674 optimizations (TNA extraction, sensitivity, LFA, …).

675 SHERLOCK4AAT profiling in Guinea and Côte d'Ivoire.

676 Trypanosome species identification can be used to finely map the risk of AAT parasite
677 transmission in these areas. After cattle, pigs are the main domestic hosts infected by
678 animal trypanosomes, but they can also be reservoirs of *T. b. gambiense. T. b.*
679 *gambiense* infections in pigs are frequently reported in Sub-Saharan Africa
680 (***Ebhodaghe et al., 2018; Okello et al., 2022a***) and these domestic animals likely
681 represent an underestimated reservoir of human-infective parasites *(**Büscher et al.,***
682 ***2018; Mehlitz and Molyneux, 2019**)*. This is all the more important than pigs are often
683 raised in close proximity to humans, increasing the risk of animal to human
684 trypanosome transmission, reinforcing our efforts to integrate the detection of both
685 animal and human parasites in domestic pigs in a One Health perspective (***Rotureau***
686 ***et al., 2022***).

687 In blood samples from Ivorian pigs, analyses with the SHERLOCK4AAT toolbox
688 revealed 37.9 % positive samples for *Trypanozoon* RNAs and 23.2 % positive samples
689 for *T. congolense* RNAs*,* with 15.2 % samples positive for both tests. In addition, no
690 sample was positive for *T. vivax, T. theileri* or *T. simiae*, but one sample was positive
691 in the *T. suis* assay and another positive for *T. b. gambiense*. These findings are
692 consistent with the most recent known distribution of animal trypanosomes in free-
693 ranging pigs raised in Côte d'Ivoire's historical gHAT foci. The use of conventional
694 molecular diagnostics on 97 free-range pigs resulted in an overall positivity rate of 57 %
695 for *Trypanozoon* DNA (PCR-TBR) and 24 % for *T. congolense forest* DNA (PCR-TCF),
696 with 14 % of pigs positive in both PCRs and none positive for *T. vivax* (PCR-TVW)
697 (***N'Djetchi et al., 2017; Traoré et al., 2021***). The epidemiological status of AAT in
698 Guinea is unclear, as no large-scale molecular studies have been published so far.
699 The blood samples from farmed pigs analysed here were collected in the prefecture of
700 N'zérékoré, a former endemic focus of gHAT. Results showed a positivity rate of
701 39.0 % for the detection of *Trypanozoon* RNAs, like that observed in Côte d'Ivoire, but
702 a lower rate of positivity for *T. congolense* RNAs (7.5 %), with 6.5 % of samples positive
703 for both tests. In addition, one sample tested positive for *T. b. gambiense,* but no *T.*
704 *vivax*, *T. simiae, T. theileri* nor *T. suis* was detected. The lack of any samples positive
705 for *T. vivax or T. theileri* in any study areas confirms that pigs are not frequent carriers

706 of these species (***Fetene et al., 2021***). However, the blood samples positive for *T. b.*
707 *gambiense* in each study site provide further evidence of the ability of pigs to carry
708 human trypanosomes and to act as potential reservoir. Similarly, the presence of *T. b.*
709 *gambiense* genetic material in pig samples has already been suspected in Côte d'Ivoire
710 (***Traoré et al., 2021***).

711 In both sites, a high prevalence of trypanosomatid parasites was observed using the
712 multiplex pan-trypanosomatid and/or pan-*Trypanozoon* assays (42.0 % in Côte d'Ivoire
713 and 48.5 % in Guinea). Having partially deconvolved the species present in these
714 animals; there is still a small proportion (8.7 % in Côte d'Ivoire and 9.5 % in Guinea) of
715 trypanosomatid parasites that remained uncharacterised by our tests on samples
716 found only positive in the multiplex pan-trypanosomatid SHERLOCK assay. Firstly,
717 these assays were designed by *in silico* determination of the most specific and
718 conserved region to target the entire Trypanosomatidae family, and even
719 Kinetoplastea class, or to discriminate between species, yet the limited number of
720 sequences available for some species in the literature and in the online databases may
721 under-represent the real genetic diversity of these parasites *in natura*. In line with this
722 hypothesis, there may also exist uncharacterised trypanosome species circulating
723 among these reservoirs, as described in small mammals in central and East Africa
724 (***Votypka et al., 2022***), and that were only detected by the broad multiplex pan-
725 trypanosomatid assay. Altogether, these results are consistent with those reported in
726 the few available previous studies (***N'Djetchi et al., 2017; Traoré et al., 2021***) and
727 confirm the effectiveness of the SHERLOCK4AAT toolbox in analysing the distribution
728 of trypanosomes in hypo-endemic gHAT foci. During natural infections, trypanosome
729 nucleic acids can be detected in the skin, adipose tissue and various organs even if
730 the blood remains negative (***Amisigo et al., 2024***). Trypanosome DNA also persists
731 in blood and skin, even after drug treatment (***Ekloh et al., 2023***). Hence, applying
732 SHERLOCK detection on skin samples in the future would be useful for monitoring
733 both blood and skin-dwelling parasites. The future development of multiplexed assays
734 combined with adapted lateral flow tests would also be highly desirable for reaching
735 field-applicable point-of-care molecular diagnostic versions of the tests useable in the
736 field. The absence of point of care diagnostic test for AAT is currently a major hurdle
737 for its surveillance and control (***Desquesnes et al., 2022b***).

738 *T. b. gambiense* is suspected to circulate among domestic animals raised in close
739 contact to humans, such as pigs. Here, *T. b. gambiense* has been detected in one
740 animal in each study site. Considering the resulting low prevalence of *T. b. gambiense*
741 infections in these two populations of domestic pigs (0.45 ± 0.9 % in Côte d'Ivoire to
742 0.50 ± 1.0 % in Guinea) and the short life expectancy of domestic pigs reared for
743 commercial purposes in these two rural areas (6 to 8 months), these animals do likely
744 not represent a significant risk to the elimination of gHAT. This is apparently confirmed
745 by the absence of new human cases as well as by the low abundance of tsetse flies in
746 the two sites (article in preparation). However, because of their proximity to humans
747 and their easy access for frequent sampling, pigs could be used as sentinels to monitor
748 *T. b. gambiense* circulation, possibly with the SHERLOCK4AAT toolbox.

749 **Acknowledgements**
750 The authors thank Annette MacLeod (University of Glasgow, Glasgow, UK) for
751 providing RNA from *T. b. rhodesiense*, Nick Van Reet and Philippe Büscher (Institute
752 of Tropical Medicine [ITM], Antwerp, Belgium) for providing RNA from *T. equiperdum*,
753 *T. evansi* types A and B, Gerald Spaeth and Artur Scherf (Institut Pasteur, Paris,
754 France) for providing RNA from *Leishmania major* and *Plasmodium falciparum* and
755 John Kelly (The London School of Hygiene & Tropical Medicine, London, UK) for
756 providing RNA from *T. cruzi*. We warmly thank all the colleagues at the University Jean
757 Lorougnon Guédé (Daloa, Côte d'Ivoire) and at the Institut Pierre Richet (Bouaké, Côte
758 d'Ivoire) as well as all the health workers in the districts of Sinfra and Bonon (Côte
759 d'Ivoire) and N'zérékoré (Guinée) for their strong support in the field.

760 **Funding**
761 This project was funded by the Agence Nationale pour la Recherche (ANR-21-CE17-
762 0022-01 SherPa), the Programme Investissement d'Avenir of the French Government
763 through the two Laboratoires d'Excellence, ANR-10-LABX-62-IBEID and ANR-11-
764 LABX-0024-PARAFRAP, and the Pasteur Network (Bourse Calmette-Yersin to AC).

765 **Author contributions**
766 RE, EPA, AC, LG and BR conceived and designed the experiments. RE, EPA, AC,
767 SB, ADH, MND, MT, YL, BD, ADC, MK, VJ and JMB performed the experiments. RE,
768 EPA, AC, PC, LG and BR analysed the data. MK, DK, MC, VJ, ST, JMB, BR and LG

769 contributed reagents, materials and analysis tools. RE, EPA, AC, LG and BR wrote the
770 manuscript. MND, MK, VJ, ST, and JMB reviewed the manuscript.

771 **Figure legends**

772 **Figure 1.** Pan and species-specific SHERLOCK assays for human and animal African
773 trypanosome infections. (A) Schematic of the target regions used in the
774 SHERLOCK4AAT toolbox. *T. congolense*, *T. theileri* (multiplex), *T. simiae*, Pan-
775 *Trypanozoon* and Pan-trypanosomatid SHERLOCK assays were designed using the
776 *18S rRNA* gene as a target; *T. vivax* SHERLOCK assay using the *IFX* gene and *T.*
777 *suis* test using the *gGAPDH* gene. Gene specific accession number in brackets below
778 the assay name. Details of the regions amplified are provided for each SHERLOCK
779 assay (amplicon). RPA primers are represented by black arrows, the extension in the
780 forward primer represents the T7 polymerase promoter sequence. The regions
781 targeted by the crRNAs (CRISPR guides) are also indicated in the diagram. The
782 schematic representation is to scale. (B) Evaluation of the specificity of single pan-
783 trypanosomatid and pan-*Trypanozoon* SHERLOCK tests RNA from *T. b. brucei* (*Tbb*),
784 *T. b. gambiense* (*Tbg*), *T. b. rhodesiense (Tbr*), *T. evansi* A (*Tev*A) and B (*Tev*B), *T.*
785 *equiperdum* (*Teq*) *T. congolense* (*Tcg*), *T. vivax* (*Tvx*), *T. theileri* (*Tth*), *Leishmania*
786 *major* (*Lm*), *Plasmodium falciparum* (*Pfl*) and HEK cells. The boxplot means are
787 represented by single lines, and error bars correspond to minimum and maximum
788 values. N=3 for the RPA amplifications and three Cas-13a detections for each RPA
789 amplification, totalling 9 replicates for each assay. *T. theileri* was used in fewer
790 replicates as an input due to the limited genetic material available. (C) Evaluation of
791 the specificity of *T. congolense*, *T. vivax*, *T. theileri*, *T. simiae* and *T. suis*-specific
792 SHERLOCK tests on RNA from *Tbb*, *Tbg*, *Tcg*, *Tvx*, *Tth*. Synthetic controls for *T.*
793 *simiae* (*Tsm*) and *T. suis* (*Tsu*) were used to evaluate the species-specificity of the
794 assays. N=1 RPA amplification and three Cas-13a detections totalling 3 replicates for
795 each assay. Error bars represent standard deviations from the mean of the replicates.
796 All inputs were used at a concentration of 5 ng/µL.

797 **Figure 2.** Evaluation of the sensitivity of SHERLOCK assays targeting trypanosome
798 species causing AAT. (A) Limit of detection (LoD) assays for the single pan-
799 trypanosomatid, pan-*Trypanozoon*, *T. vivax, T. congolense and T. theileri* assays were
800 performed using RNAs from bloodstream parasites diluted to obtain equivalent
801 concentrations of parasites per mL, ranging from 10^7 to 0.1 parasites/mL. (B) LoD of

802 *T. simiae* and *T. suis* assays were performed on consecutive dilutions of the synthetic
803 controls, ranging from 10^{10} to 10^{1} fM. N=24 for pan-trypanosomatid assay, N=12 for
804 pan-*Trypanozoon* and *T. theileri* assays, N=6 for *T. simiae* assay and N=3 for *T.*
805 *congolense, T. vivax* and *T. suis* assays. Error bars represent standard deviations from
806 the mean of the replicates; open circle represents each replicate.

807 **Figure 3**. Comparison of the single and multiplex 18S pan-trypanosomatid
808 SHERLOCK assays efficiency. (A) Schematic of the single (one crRNA) and multiplex
809 (two crRNAs) pan-trypanosomatid SHERLOCK assays designed using the *18S rRNA*
810 gene as a target. Gene specific accession number in brackets below the assay name.
811 Details of the amplified gene regions are provided (amplicon). RPA primers are
812 represented by black arrows; the forward primer extension represents the T7
813 polymerase promoter sequence. The regions targeted by the crRNAs are indicated in
814 the diagram. (B) Posterior sensitivity estimates of the single (green) and multiplex
815 (purple) pan-trypanosomatid SHERLOCK assays on the 224 pig blood samples from
816 Côte d'Ivoire presented in Figure 4. Estimates were obtained with the Monte Carlo
817 method (Gibbs sampling) proceeding in an iterative chain. (C) Results of pan-
818 *Trypanozoon* SHERLOCK assay plotted against results of the single (left panel) and
819 multiplex (right panel) 18S pan-trypanosomatid SHERLOCK assays on pig samples
820 from Côte d'Ivoire. The coloured dashed lines represent the detection thresholds set
821 for each of the tests: single pan-trypanosomatid (green), multiplex pan-trypanosomatid
822 (purple), and pan-*Trypanozoon* (orange). Numbers and proportions (%) of double
823 positive samples are indicated at the top right of each graph and only positive for pan-
824 trypanosomatid in the bottom right part of each graph.

825 **Figure 4.** Diversity of blood trypanosomatids among free-range pigs from Côte d'Ivoire
826 assessed by the SHERLOCK4AAT toolbox. (A) Map of the Côte d'Ivoire, the region
827 where the samples were collected is highlighted in purple. (B) Results of the
828 SHERLOCK4AAT screening of 224 pig samples collected in Côte d'Ivoire. The
829 coloured dashed lines represent the detection thresholds set for each assay. Each
830 colour represents a specific test: multiplex pan-trypanosomatid (green), pan-
831 *Trypanozoon* (orange), *T. b. gambiense* (yellow), *T. congolense* (light green), *T. vivax*
832 (purple), *T. theileri* (red), *T. simiae* (blue) and *T. suis* (black). (C) Table summarizing
833 the number of positive samples as well as the percentage (%) positive infections for
834 each test, calculated on the total number of samples analysed. The total number of

835 samples analysed were 219 for the multiplex pan-trypanosomatid assay, 173 for the
836 *T. vivax*-specific assay, and 224 for all other SHERLOCK assays. (D) Venn diagram
837 representing the crossover between the positive samples analysed with the three tests
838 (multiplex pan-trypanosomatid (green), pan-*Trypanozoon* (orange) and *T. congolense*
839 (purple)) giving the highest prevalence. The percentage of the total is shown in
840 brackets below the number of samples constituting each fraction.

841 **Figure 5.** Diversity of blood trypanosomatids among farm pigs from Guinea assessed
842 by the SHERLOCK4AAT toolbox. (A) Map of Guinea showing the N'zérékoré
843 prefecture where samples were collected in pink. (B) Results of the SHERLOCK4AAT
844 screening of 200 pig samples collected in Guinea. The coloured dashed lines represent
845 the detection thresholds set for each of the tests. Each colour represents a specific
846 test: multiplex pan-trypanosomatid (green), pan-*Trypanozoon* (orange), *T. b.*
847 *gambiense* (yellow), *T. congolense* (light green), *T. vivax* (purple), *T. theileri* (red), *T.*
848 *simiae* (blue) and *T. suis* (black). (C) Table summarizing the number of positive
849 samples as well as the percentage (%) positive infections for each test, calculated on
850 the total number of samples analysed (n=200). (D) Venn diagram representing the
851 crossover between the positive samples analysed with the three tests (multiplex pan-
852 trypanosomatid (green), pan-*Trypanozoon* (orange) and *T. congolense* (purple)) giving
853 the highest prevalence. The percentage of the total is shown in brackets below the
854 number of samples constituting each fraction.

855 **Supplementary figure legends**

856 **Supplementary Figure 1.** A: Representation of the proportions of identity between
857 *18S rRNA* (A) and *GAPDH* (B) genes from Microsporidia, Ciliophora, Haemosporida,
858 Diplomonadida, Symbiontida, Diplonemea, Euglenida and Kinetoplastea, focusing on
859 several species within last family.

860 **Supplementary Figure 2.** (A) Alignments for 18S Pan-trypanosomatid SHERLOCK
861 target region. The sequences used for the alignments are as follows: Microsporidia
862 (*Nosema adalia*, KC412706.1), Ciliophora (*Vorticella sp.*, DQ487201.2),
863 Haemosporida (*Plasmodium falciparum*, XR_002966679.1), Diplomonadida (*Giargia*
864 *intestinalis*, XR_005248679.1), Symbiontida (*Calkinsia aureus*, EU753419.1),
865 Diplonemea (*Diplonema ambulator*, AY425009.1), Euglenida (*Euglena sanguinea*,
866 JQ281806.1) and Kinetoplastea (*Trypanosoma* (*T*) *brucei brucei*, XR_002989632.1).

867 (B) Alignments for 18S Pan-*Trypanozoon* SHERLOCK target region. The sequences
868 used for the alignments are as follows: Human (H, pdb|5VYC|i), *Plasmodium*
869 *falciparum* (Pfl, XR_002966679.1), *Leishmania major* (Lm, GQ332361.1), *T. cruzi*
870 (Tcz, AJ009147.1), *T. vivax* (Tvx, EU477537.1), *T. congolense* (Tcg, AJ009146.1), *T.*
871 *theileri* (Tth, AJ009163.1), *T. simiae* (Tsm, AJ404608.1), *T. suis* (Tsu, MK962702.1)
872 and *T. brucei brucei* (Tbb, XR_002989632.1). Non-conserved bases between
873 sequences are highlighted in bold.

874 **Supplementary Figure 3.** Summary of BLAST analysis obtained against the 18S pan-
875 trypanosomatid SHERLOCK amplicon and evaluation of the homology of the target
876 region of each crRNA. The percentage identity of the target amplicon of pan-
877 trypanosomatid RPA was evaluated using different degrees of exclusion, to assess its
878 percentage of identity within the different groups and especially in the Phylum
879 Euglenozoa, excluding the target group Kinetoplastea. The number of sequences
880 evaluated is shown, as well as the percentage of sequences where the target regions
881 of the pan-trypanosomatid guides (crRNAs) are conserved.

882 **Supplementary Figure 4.** Screening of different RPA pairs of primers and/or crRNAs
883 guides for each SHERLOCK assay optimization. In each evaluation a positive control
884 (RNA from a target species, coloured bar) and a negative control (RNA from a non-
885 target species, grey bar) were used. RPA pairs of primers are named A, B or C, while
886 crRNAs were name from 1 to 10. The time point used is indicated. # indicates the
887 combination of RPA primers and crRNA selected for the rest of the analysis. All inputs
888 were used at a concentration of 5 ng/µL.

889 **Supplementary Figure 5.** Alignments of the 18S *T. congolense* SHERLOCK target
890 region. The sequences used for the alignments are from *T. simiae*, *T. godfreyi*, *T.*
891 *sapaensis*, *T. vivax*, *T. theileri* and *T. thomasbancrofti*. Non-conserved bases between
892 sequences are highlighted in grey. The percentage identity of each sequence was
893 analysed against the RPA amplicon in the *T. congolense*-specific SHERLOCK assay.

894 **Supplementary Figure 6**. Comparison of the limit of detection of the single and
895 multiplex 18S pan-trypanosomatid SHERLOCK assays. Single and multiplex 18S pan-
896 trypanosomatid SHERLOCK assays on dilutions of *T. b. brucei* RNA and on RNA
897 extracted from HEK human cells as negative control. N=9 for each dilution. Error bars
898 represent standard deviations from the mean of the replicates.

899 **Supplementary Figure 7**. Background cross-reactivity of the 18S pan-trypanosomatid
900 (A) and 18S pan-*Trypanozoon* (B) SHERLOCK assays using genetic material
901 extracted from pig blood as input. Means are represented by single lines. Quantities of
902 porcine and *T. b. brucei* genetic material extracts included in each trial are as follows:
903 "-" none, "+" 1 ng/µL, "++" 2 ng/µL and "+++" 3 ng/µL.

904 **Supplementary Figure 8.** Threshold determination for all new SHERLOCK4AAT
905 assays. (A) Compilation of positive and negative results obtained using multiplex pan-
906 trypanosomatid and pan-*Trypanozoon* SHERLOCK tests and ROC curves obtained for
907 each analysis. The red dotted line marks the selected threshold for each test. (B)
908 Compilation of positive and negative results obtained using the species-specific
909 SHERLOCK assays and ROC curve obtained for each analysis. The red dotted line
910 marks the selected threshold for each test. (C) Summary of the analytical features of
911 each SHERLOCK assay. Analytical sensitivity (95 % of CI), specificity (95 % of CI) and
912 fold change cut-off.

913 **Supplementary Figure 9.** Posterior sensitivity estimates of three SHERLOCK assays
914 (multiplex pan-trypanosomatid, pan-*Trypanozoon* and *T. congolense*-specific
915 SHERLOCK assays, red curve) to the three parasitological tests (buffy coat
916 examination, mAECT and /or isolation in mice, orange curve) performed in parallel on
917 the 224 pig blood samples from Côte d'Ivoire. Estimates were obtained with the Monte
918 Carlo method (Gibbs sampling) proceeding in an iterative chain.

919 **Supplementary Table 1.** Accession numbers of organisms used to evaluate the
920 presence of single nucleotide polymorphism (SNPs) in the different target regions.

921 **Supplementary Table 2.** Primers and crRNA guides used for the SHERLOCK4AAT
922 toolbox.

923 **Supplementary Table 3.** RPA primers used to produce the *in vitro* transcribed targets
924 (positive control templates).

925 **References**

926 **Álvarez-Rodríguez A**, Jin B-K, Radwanska M, Magez S. 2022. Recent progress in
927 diagnosis and treatment of Human African Trypanosomiasis has made the
928 elimination of this disease a realistic target by 2030. *Frontiers in medicine*
929 **9**:1037094. doi: 10.3389/fmed.2022.1037094.

930 **Amisigo CM**, Amegatcher G, Sunter JD, Gwira TM. 2024. Adipose and skin
931 distribution of African trypanosomes in natural animal infections. *Parasites & vectors*
932 **17**:215. doi: 10.1186/s13071-024-06277-7.
933 **Autheman D**, Crosnier C, Clare S, Goulding DA, Brandt C, Harcourt K, Tolley C,
934 Galaway F, Khushu M, Ong H, Romero-Ramirez A, Duffy CW, Jackson AP, Wright
935 GJ. 2021. An invariant Trypanosoma vivax vaccine antigen induces protective
936 immunity. *Nature* **595**:96–100. doi: 10.1038/s41586-021-03597-x.
937 **Barrett MP**, Priotto G, Franco JR, Lejon V, Lindner AK. 2024. Elimination of human
938 African trypanosomiasis: The long last mile. *PLoS neglected tropical diseases*
939 **18**:e0012091. doi: 10.1371/journal.pntd.0012091.
940 **Boulangé A**, Lejon V, Berthier D, Thévenon S, Gimonneau G, Desquesnes M, Abah
941 S, Agboho P, Chilongo K, Gebre T, Fall AG, Kaba D, Magez S, Masiga D, Matovu
942 E, Moukhtar A, Neves L, Olet PA, Pagabeleguem S, Shereni W, Sorli B, Taioe MO,
943 Tejedor Junco MT, Yagi R, Solano P, Cecchi G. 2022. The COMBAT project:
944 controlling and progressively minimizing the burden of vector-borne animal
945 trypanosomosis in Africa. *Open research Europe* **2**:67.
946 doi: 10.12688/openreseurope.14759.2.
947 **Brotánková A**, Fialová M, Čepička I, Brzoňová J, Svobodová M. 2022. Trypanosomes
948 of the Trypanosoma theileri Group: Phylogeny and New Potential Vectors.
949 *Microorganisms* **10**. doi: 10.3390/microorganisms10020294.
950 **Brown LD**, Cai TT, DasGupta A. 2001. Interval Estimation for a Binomial Proportion.
951 *Statistical Science* **16**. doi: 10.1214/ss/1009213286.
952 **Budd LT**. 2001. Trypanosomosis, Tsestse and Africa.
953 https://assets.publishing.service.gov.uk/media/57a08d23e5274a31e0001686/ZC01
954 35a.pdf.
955 **Büscher P**, Bart J-M, Boelaert M, Bucheton B, Cecchi G, Chitnis N, Courtin D,
956 Figueiredo LM, Franco J-R, Grébaut P, Hasker E, Ilboudo H, Jamonneau V, Koffi M,
957 Lejon V, MacLeod A, Masumu J, Matovu E, Mattioli R, Noyes H, Picado A, Rock KS,
958 Rotureau B, Simo G, Thévenon S, Trindade S, Truc P, van Reet N. 2018. Do Cryptic
959 Reservoirs Threaten Gambiense-Sleeping Sickness Elimination? *Trends in*
960 *parasitology* **34**:197–207. doi: 10.1016/j.pt.2017.11.008.
961 **Claes F**, Radwanska M, Urakawa T, Majiwa PA, Goddeeris B, Büscher P. 2004.
962 Variable Surface Glycoprotein RoTat 1.2 PCR as a specific diagnostic tool for the

963 detection of Trypanosoma evansi infections. *Kinetoplastid biology and disease* **3**:3.
964 doi: 10.1186/1475-9292-3-3.
965 **Contreras Garcia M**, Walshe E, Steketee PC, Paxton E, Lopez-Vidal J, Pearce MC,
966 Matthews KR, Ezzahra-Akki F, Evans A, Fairlie-Clark K, Matthews JB, Grey F,
967 Morrison LJ. 2022. Comparative Sensitivity and Specificity of the 7SL sRNA
968 Diagnostic Test for Animal Trypanosomiasis. *Frontiers in Veterinary Science* **9**.
969 doi: 10.3389/fvets.2022.868912.
970 **Courtin F**, Camara O, Camara M, Kagbadouno M, Bucheton B, Solano P, Jamonneau
971 V. 2019. Maladie du sommeil dans le foyer historique de Guinée forestière :
972 actualisation grâce à une méthode géographique. *Parasite (Paris, France)* **26**:61.
973 doi: 10.1051/parasite/2019061.
974 **Deborggraeve S**, Claes F, Laurent T, Mertens P, Leclipteux T, Dujardin JC, Herdewijn
975 P, Büscher P. 2006. Molecular dipstick test for diagnosis of sleeping sickness.
976 *Journal of clinical microbiology* **44**:2884–2889. doi: 10.1128/JCM.02594-05.
977 **Desquesnes M**, Gonzatti M, Sazmand A, Thévenon S, Bossard G, Boulangé A,
978 Gimonneau G, Truc P, Herder S, Ravel S, Sereno D, Jamonneau V, Jittapalapong
979 S, Jacquiet P, Solano P, Berthier D. 2022a. A review on the diagnosis of animal
980 trypanosomoses. *Parasites & vectors* **15**:64. doi: 10.1186/s13071-022-05190-1.
981 **Desquesnes M**, Sazmand A, Gonzatti M, Boulangé A, Bossard G, Thévenon S,
982 Gimonneau G, Truc P, Herder S, Ravel S, Sereno D, Waleckx E, Jamonneau V,
983 Jacquiet P, Jittapalapong S, Berthier D, Solano P, Hébert L. 2022b. Diagnosis of
984 animal trypanosomoses: proper use of current tools and future prospects. *Parasites*
985 *& vectors* **15**:235. doi: 10.1186/s13071-022-05352-1.
986 **Ebhodaghe F**, Ohiolei JA, Isaac C. 2018. A systematic review and meta-analysis of
987 small ruminant and porcine trypanosomiasis prevalence in sub-Saharan Africa (1986
988 to 2018). *Acta tropica* **188**:118–131. doi: 10.1016/j.actatropica.2018.08.034.
989 **Ekloh W**, Sunter JD, Gwira TM. 2023. African trypanosome infection patterns in cattle
990 in a farm setting in Southern Ghana. *Acta tropica* **237**:106721.
991 doi: 10.1016/j.actatropica.2022.106721.
992 **Fetene E**, Leta S, Regassa F, Büscher P. 2021. Global distribution, host range and
993 prevalence of Trypanosoma vivax: a systematic review and meta-analysis. *Parasites*
994 *& vectors* **14**:80. doi: 10.1186/s13071-021-04584-x.
995 **Franco JR**, Priotto G, Paone M, Cecchi G, Ebeja AK, Simarro PP, Sankara D, Metwally
996 SBA, Argaw DD. 2024. The elimination of human African trypanosomiasis:

997 Monitoring progress towards the 2021-2030 WHO road map targets. *PLoS neglected*
998 *tropical diseases* **18**:e0012111. doi: 10.1371/journal.pntd.0012111.
999 **Giordani F**, Morrison LJ, Rowan TG, Koning HP de, Barrett MP. 2016. The animal
1000 trypanosomiases and their chemotherapy: a review. *Parasitology* **143**:1862–1889.
1001 doi: 10.1017/S0031182016001268.
1002 **Gootenberg JS**, Abudayyeh OO, Lee JW, Essletzbichler P, Dy AJ, Joung J, Verdine
1003 V, Donghia N, Daringer NM, Freije CA, Myhrvold C, Bhattacharyya RP, Livny J,
1004 Regev A, Koonin EV, Hung DT, Sabeti PC, Collins JJ, Zhang F. 2017. Nucleic acid
1005 detection with CRISPR-Cas13a/C2c2. *Science (New York, N.Y.)* **356**:438–442.
1006 doi: 10.1126/science.aam9321.
1007 **Holland WG**, Claes F, My LN, Thanh NG, Tam PT, Verloo D, Büscher P, Goddeeris
1008 B, Vercruysse J. 2001. A comparative evaluation of parasitological tests and a PCR
1009 for Trypanosoma evansi diagnosis in experimentally infected water buffaloes.
1010 *Veterinary parasitology* **97**:23–33. doi: 10.1016/S0304-4017(01)00381-8.
1011 **Joseph L**, Gyorkos TW, Coupal L. 1995. Bayesian estimation of disease prevalence
1012 and the parameters of diagnostic tests in the absence of a gold standard. *American*
1013 *journal of epidemiology* **141**:263–272. doi: 10.1093/oxfordjournals.aje.a117428.
1014 **Karshima SN**, Lawal IA, Bata SI, Barde IJ, Adamu PV, Salihu A, Dross PN, Obalisa
1015 A. 2016. Animal reservoirs of Trypanosoma brucei gambiense around the old Gboko
1016 sleeping sickness focus in Nigeria. *Journal of parasitology and vector biology*.
1017 **Kellner MJ**, Koob JG, Gootenberg JS, Abudayyeh OO, Zhang F. 2019. SHERLOCK:
1018 nucleic acid detection with CRISPR nucleases. *Nature protocols* **14**:2986–3012.
1019 doi: 10.1038/s41596-019-0210-2.
1020 **Kristjanson PM**, Swallow BM, Rowlands GJ, Kruska RL, Leeuw PN de. 1999.
1021 Measuring the costs of African animal trypanosomosis, the potential benefits of
1022 control and returns to research. *Agricultural Systems* **59**:79–98. doi: 10.1016/S0308-
1023 521X(98)00086-9.
1024 **Magang EMK**, Kamga RMN, Telleria J, Tichit M, Crouzols A, Kaboré J, Hardy D,
1025 Bouaka CUT, Jamonneau V, Rotureau B, Kuete V, Bart J-M, Simo G. 2023.
1026 Prevalence of blood and skin trypanosomes in domestic and wild fauna from two
1027 sleeping sickness foci in Southern Cameroon. *PLoS neglected tropical diseases*
1028 **17**:e0011528. doi: 10.1371/journal.pntd.0011528.

1029 **McGinnis S**, Madden TL. 2004. BLAST: at the core of a powerful and diverse set of
1030 sequence analysis tools. *Nucleic acids research* **32**:W20-5.
1031 doi: 10.1093/nar/gkh435.
1032 **Mehlitz D**, Molyneux DH. 2019. The elimination of Trypanosoma brucei gambiense?
1033 Challenges of reservoir hosts and transmission cycles: Expect the unexpected.
1034 *Parasite epidemiology and control* **6**:e00113. doi: 10.1016/j.parepi.2019.e00113.
1035 **Meyer A**, Holt HR, Selby R, Guitian J. 2016. Past and Ongoing Tsetse and Animal
1036 Trypanosomiasis Control Operations in Five African Countries: A Systematic
1037 Review. *PLoS neglected tropical diseases* **10**:e0005247.
1038 doi: 10.1371/journal.pntd.0005247.
1039 **Morrison LJ**, Tait A, McCormack G, Sweeney L, Black A, Truc P, Likeufack ACL,
1040 Turner CM, MacLeod A. 2008. Trypanosoma brucei gambiense Type 1 populations
1041 from human patients are clonal and display geographical genetic differentiation.
1042 *Infection, genetics and evolution : journal of molecular epidemiology and*
1043 *evolutionary genetics in infectious diseases* **8**:847–854.
1044 doi: 10.1016/j.meegid.2008.08.005.
1045 **N'Djetchi MK**, Camara O, Koffi M, Camara M, Kaba D, Kaboré J, Tall A, Rotureau B,
1046 Glover L, Traoré MB, Koné M, Coulibaly B, Adingra GP, Soumah A, Gassama M,
1047 Camara AD, Compaoré CFA, Camara A, Boiro S, Anton EP, Bessell P, van Reet N,
1048 Bucheton B, Jamonneau V, Bart J-M, Solano P, Biéler S, Lejon V. 2024. Specificity
1049 of serological screening tests and reference laboratory tests to diagnose gambiense
1050 human African trypanosomiasis: a prospective clinical performance study. *Infectious*
1051 *diseases of poverty* **13**:53. doi: 10.1186/s40249-024-01220-5.
1052 **N'Djetchi MK**, Ilboudo H, Koffi M, Kaboré J, Kaboré JW, Kaba D, Courtin F, Coulibaly
1053 B, Fauret P, Kouakou L, Ravel S, Deborggraeve S, Solano P, Meeûs T de, Bucheton
1054 B, Jamonneau V. 2017. The study of trypanosome species circulating in domestic
1055 animals in two human African trypanosomiasis foci of Côte d'Ivoire identifies pigs
1056 and cattle as potential reservoirs of Trypanosoma brucei gambiense. *PLoS*
1057 *neglected tropical diseases* **11**:e0005993. doi: 10.1371/journal.pntd.0005993.
1058 **Okello I**, Mafie E, Eastwood G, Nzalawahe J, Mboera LEG. 2022a. African Animal
1059 Trypanosomiasis: A Systematic Review on Prevalence, Risk Factors and Drug
1060 Resistance in Sub-Saharan Africa. *Journal of medical entomology* **59**:1099–1143.
1061 doi: 10.1093/jme/tjac018.

1062 **Okello I**, Mafie E, Eastwood G, Nzalawahe J, Mboera LEG, Onyoyo S. 2022b.
1063 Prevalence and Associated Risk Factors of African Animal Trypanosomiasis in
1064 Cattle in Lambwe, Kenya. *Journal of parasitology research* **2022**:5984376.
1065 doi: 10.1155/2022/5984376.
1066 **Piepenburg O**, Williams CH, Stemple DL, Armes NA. 2006. DNA detection using
1067 recombination proteins. *PLoS biology* **4**:e204. doi: 10.1371/journal.pbio.0040204.
1068 **Radwanska M**, Claes F, Magez S, Magnus E, Perez-Morga D, Pays E, Büscher P.
1069 2002. Novel primer sequences for polymerase chain reaction-based detection of
1070 Trypanosoma brucei gambiense. *The American journal of tropical medicine and*
1071 *hygiene* **67**:289–295. doi: 10.4269/ajtmh.2002.67.289.
1072 **Richards S**, Morrison LJ, Torr SJ, Barrett MP, Manangwa O, Mramba F, Auty H. 2021.
1073 Pharma to farmer: field challenges of optimizing trypanocide use in African animal
1074 trypanosomiasis. *Trends in parasitology* **37**:831–843. doi: 10.1016/j.pt.2021.04.007.
1075 **Rodrigues CMF**, Garcia HA, Rodrigues AC, Pereira DL, Pereira CL, Viola LB, Neves
1076 L, Camargo EP, Gibson W, Teixeira MMG. 2020. Expanding our knowledge on
1077 African trypanosomes of the subgenus Pycnomonas: A novel Trypanosoma suis-like
1078 in tsetse flies, livestock and wild ruminants sympatric with Trypanosoma suis in
1079 Mozambique. *Infection, genetics and evolution : journal of molecular epidemiology*
1080 *and evolutionary genetics in infectious diseases* **78**:104143.
1081 doi: 10.1016/j.meegid.2019.104143.
1082 **Romero-Ramirez A**, Casas-Sánchez A, Autheman D, Duffy CW, Brandt C, Clare S,
1083 Harcourt K, André MR, Almeida Castilho Neto KJG de, Teixeira MMG, Machado RZ,
1084 Coombes J, Flynn RJ, Wright GJ, Jackson AP. 2022. Vivaxin genes encode highly
1085 immunogenic, non-variant antigens on the Trypanosoma vivax cell-surface. *PLoS*
1086 *neglected tropical diseases* **16**:e0010791. doi: 10.1371/journal.pntd.0010791.
1087 **Rotureau B**, Waleckx E, Jamonneau V, Solano P, Molia S, Debré P, Dellagi K, Morand
1088 S. 2022. Enhancing research integration to improve One Health actions: learning
1089 lessons from neglected tropical diseases experiences. *BMJ global health* **7**.
1090 doi: 10.1136/bmjgh-2022-008881.
1091 **Schisterman EF**, Perkins NJ, Liu A, Bondell H. 2005. Optimal cut-point and its
1092 corresponding Youden Index to discriminate individuals using pooled blood samples.
1093 *Epidemiology (Cambridge, Mass.)* **16**:73–81.
1094 doi: 10.1097/01.ede.0000147512.81966.ba.

1095 **Serem EK**, Mburu DM, Abdullahi OA, Bargul JL. 2024. A scoping review on tsetse fly
1096 blood meal sources and its assay methods since 1956 to 2022. *Parasites & vectors*
1097 **17**:52. doi: 10.1186/s13071-023-06114-3.
1098 **Sievers F**, Higgins DG. 2018. Clustal Omega for making accurate alignments of many
1099 protein sequences. *Protein science : a publication of the Protein Society* **27**:135–
1100 145. doi: 10.1002/pro.3290.
1101 **Sima N**, Dujeancourt-Henry A, Perlaza BL, Ungeheuer M-N, Rotureau B, Glover L.
1102 2022. SHERLOCK4HAT: A CRISPR-based tool kit for diagnosis of Human African
1103 Trypanosomiasis. *EBioMedicine* **85**:104308. doi: 10.1016/j.ebiom.2022.104308.
1104 **Simo G**, Rayaisse JB. 2015. Challenges facing the elimination of sleeping sickness in
1105 west and central Africa: sustainable control of animal trypanosomiasis as an
1106 indispensable approach to achieve the goal. *Parasites & vectors* **8**:640.
1107 doi: 10.1186/s13071-015-1254-y.
1108 **Traoré BM**, Koffi M, N'Djetchi MK, Kaba D, Kaboré J, Ilboudo H, Ahouty BA, Koné M,
1109 Coulibaly B, Konan T, Segard A, Kouakou L, Meeûs T de, Ravel S, Solano P, Bart
1110 J-M, Jamonneau V. 2021. Free-ranging pigs identified as a multi-reservoir of
1111 Trypanosoma brucei and Trypanosoma congolense in the Vavoua area, a historical
1112 sleeping sickness focus of Côte d'Ivoire. *PLoS neglected tropical diseases*
1113 **15**:e0010036. doi: 10.1371/journal.pntd.0010036.
1114 **Vourchakbé J**, Tiofack ZAA, Kante TS, Mpoame M, Simo G. 2020. L'identification
1115 moléculaire de Trypanosoma brucei gambiense chez les porcs, les chiens et les
1116 petits ruminants naturellement infectés confirme les animaux domestiques comme
1117 réservoirs potentiels de la maladie du sommeil au Tchad. *Parasite (Paris, France)*
1118 **27**:63. doi: 10.1051/parasite/2020061.
1119 **Ye J**, Coulouris G, Zaretskaya I, Cutcutache I, Rozen S, Madden TL. 2012. Primer-
1120 BLAST: a tool to design target-specific primers for polymerase chain reaction. *BMC*
1121 *bioinformatics* **13**:134. doi: 10.1186/1471-2105-13-134.
1122

Figure 1

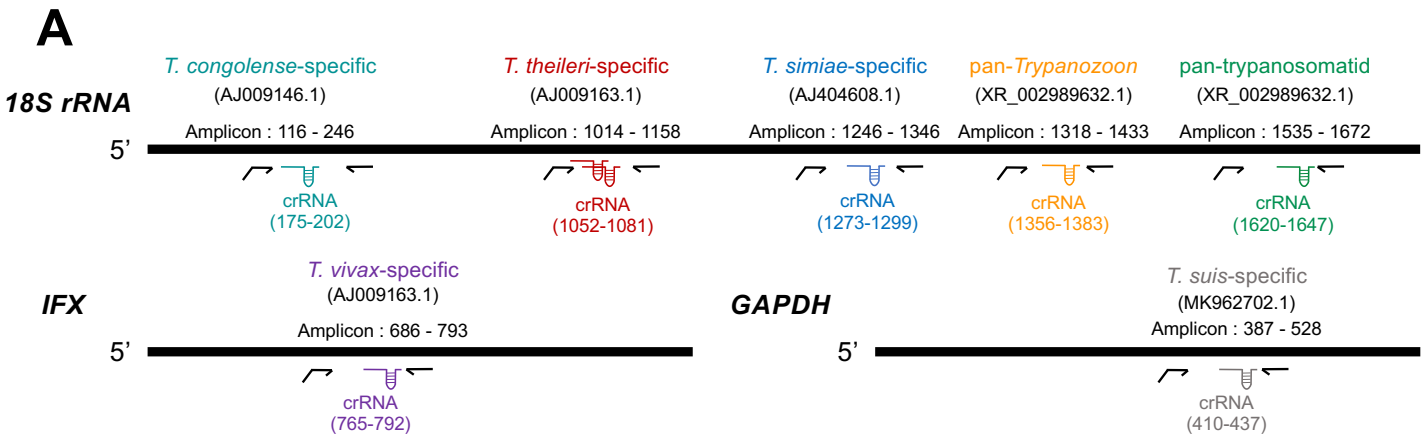
A
18S rRNA
T. congolense-specific
(AJ009146.1)
Amplicon : 116 - 246
T. theileri-specific
(AJ009163.1)
Amplicon : 1014 - 1158
T. simiae-specific
(AJ404608.1)
Amplicon : 1246 - 1346
pan-Trypanozoon
(XR_002989632.1)
Amplicon : 1318 - 1433
pan-trypanosomatid
(XR_002989632.1)
Amplicon : 1535 - 1672
5'
crRNA
(175-202)
crRNA
(1052-1081)
crRNA
(1273-1299)
crRNA
(1356-1383)
crRNA
(1620-1647)
IFX
T. vivax-specific
(AJ009163.1)
Amplicon : 686 - 793
5'
crRNA
(765-792)
GAPDH
T. suis-specific
(MK962702.1)
Amplicon : 387 - 528
5'
crRNA
(410-437)

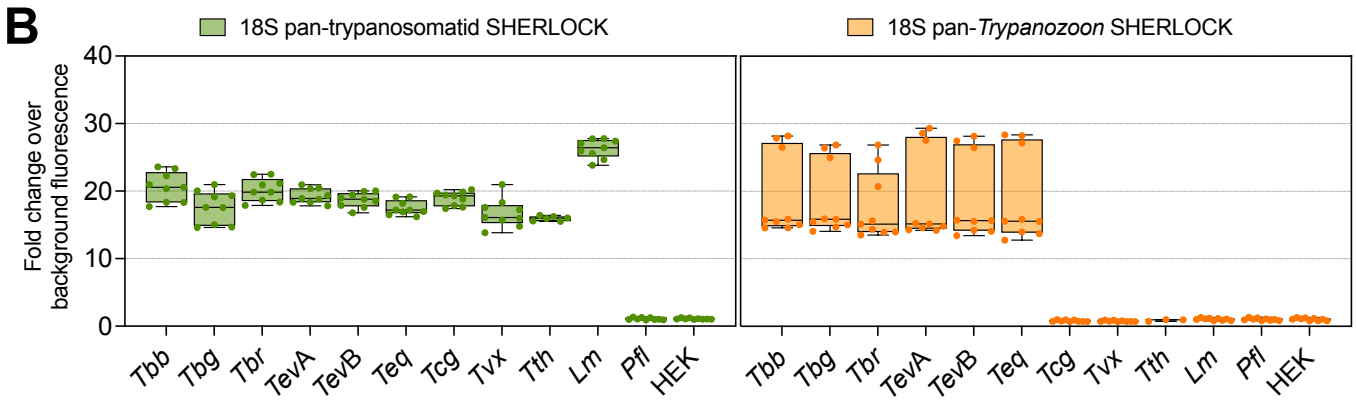
B
18S pan-trypanosomatid SHERLOCK
18S pan-Trypanozoon SHERLOCK
Fold change over background fluorescence
40
30
20
10
0
Tbb
Tbg
Tbr
TevA
TevB
Teq
Tcg
Tvx
Tth
Lm
Pfl
HEK

C
T.congolense
T.vivax
T.theileri
T.simiae
T.suis
Fold change over background fluorescence
30
20
10
0
Tbb
Tbg
Tcg
Tvx
Tth
Tsm
Tsu

Figure 2

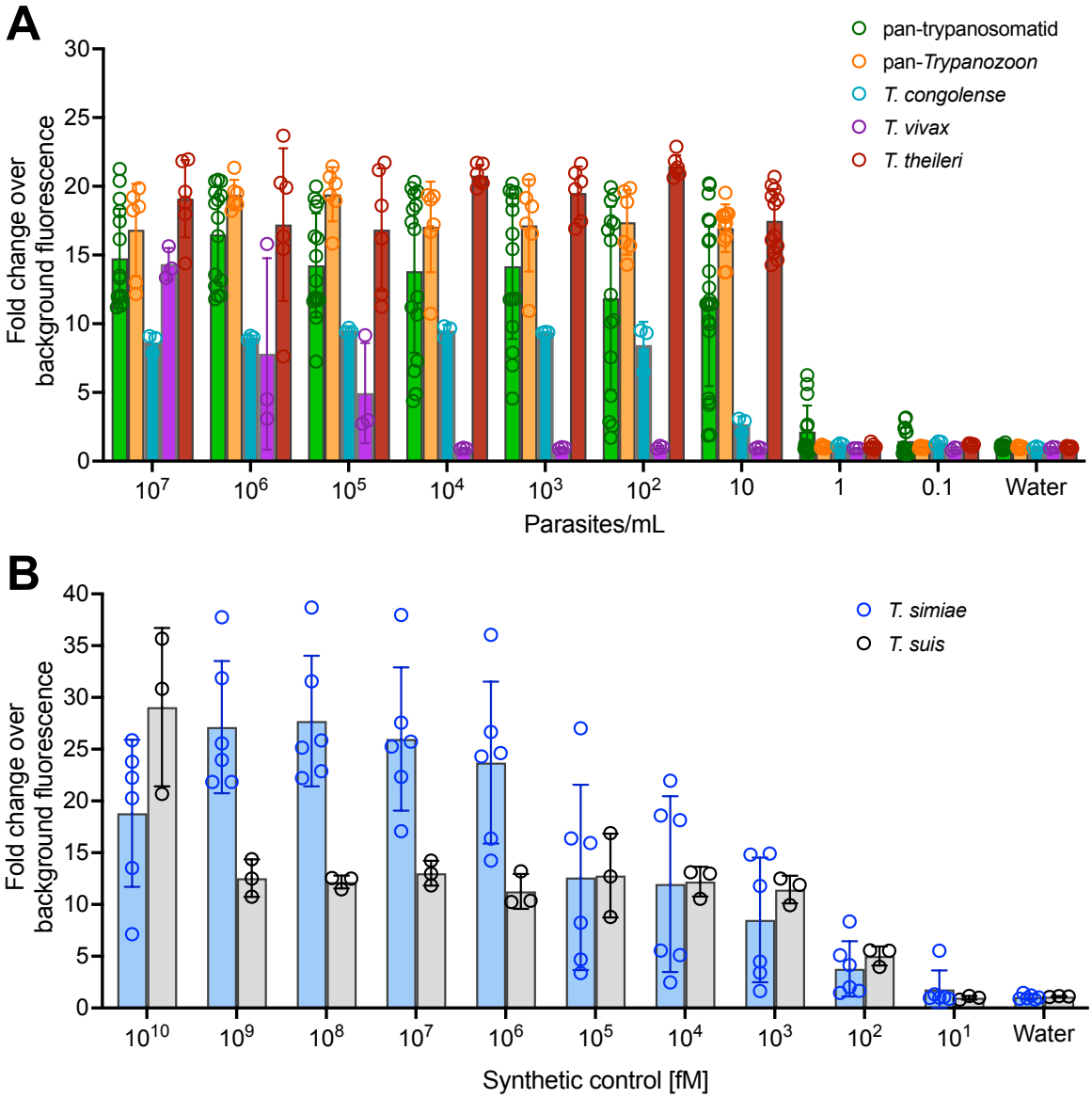
A
pan-trypanosomatid
pan-Trypanozoon
T. congolense
T. vivax
T. theileri
Fold change over background fluorescence
0
5
10
15
20
25
30
10^7
10^6
10^5
10^4
10^3
10^2
10
1
0.1
Water
Parasites/mL
B
T. simiae
T. suis
Fold change over background fluorescence
0
5
10
15
20
25
30
35
40
10^10
10^9
10^8
10^7
10^6
10^5
10^4
10^3
10^2
10^1
Water
Synthetic control [fM]

Figure 3

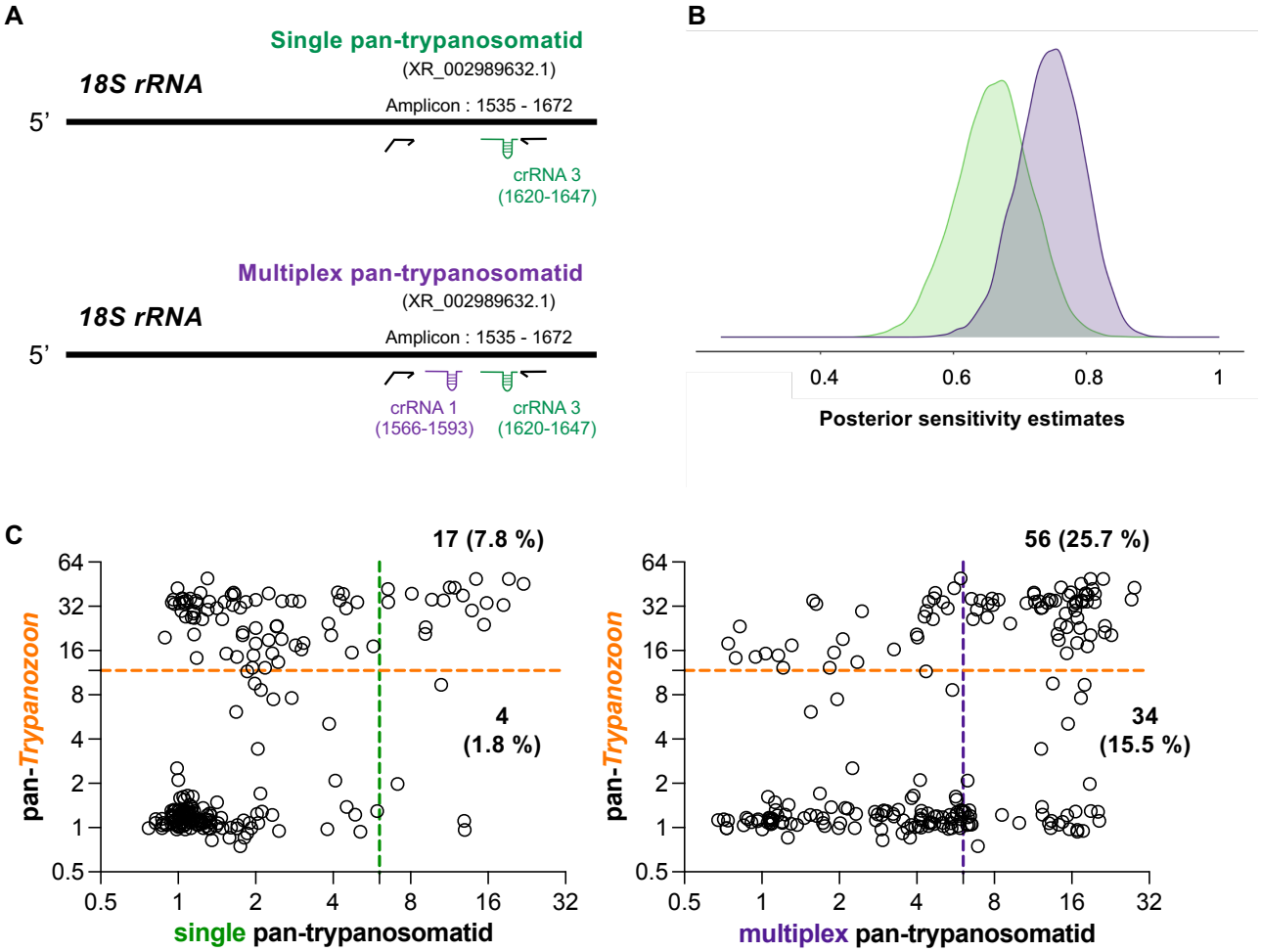
A
Single pan-trypanosomatid
(XR_002989632.1)
18S rRNA
Amplicon : 1535 - 1672
5'
crRNA 3
(1620-1647)
Multiplex pan-trypanosomatid
(XR_002989632.1)
18S rRNA
Amplicon : 1535 - 1672
5'
crRNA 1
(1566-1593)
crRNA 3
(1620-1647)
B
0.4
0.6
0.8
1
Posterior sensitivity estimates
C
17 (7.8 %)
4
(1.8 %)
pan-Trypanozoon
single pan-trypanosomatid
56 (25.7 %)
34
(15.5 %)
pan-Trypanozoon
multiplex pan-trypanosomatid

Figure 4

A

B

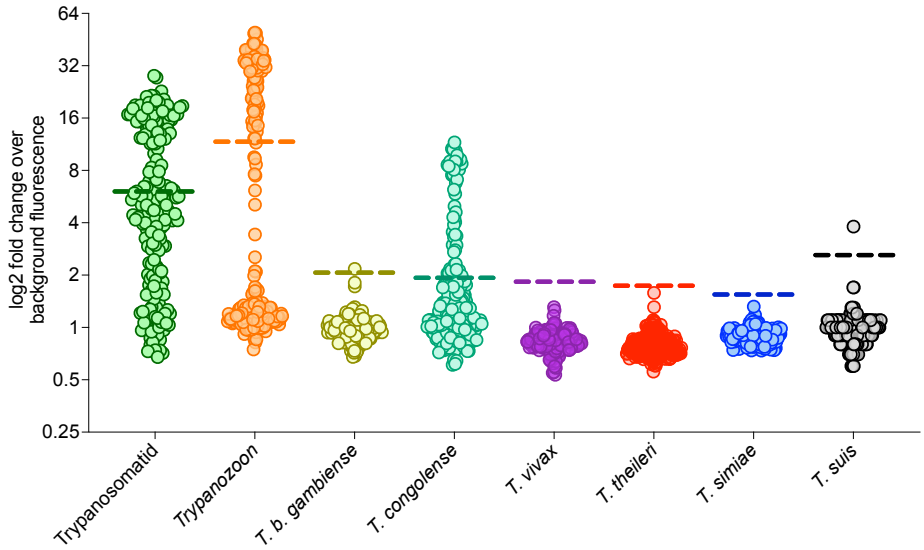

C

	No. positive samples	% infections (n=224)
Trypanosomatid	90	41.1 %
Trypanozoon	85	37.9 %
T. b. gambiense	1	0.45 %
T. congolense	52	23.2 %
T. vivax	0	0.0 %
T. theileri	0	0.0 %
T. simiae	0	0.0 %
T. suis	1	0.45 %

D

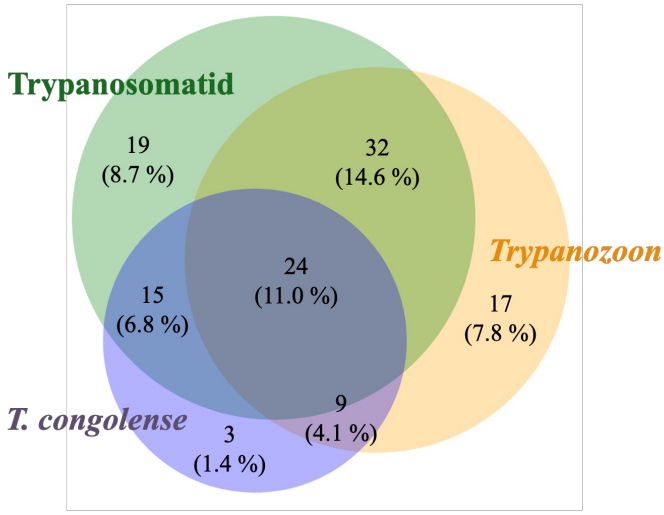

Figure 5

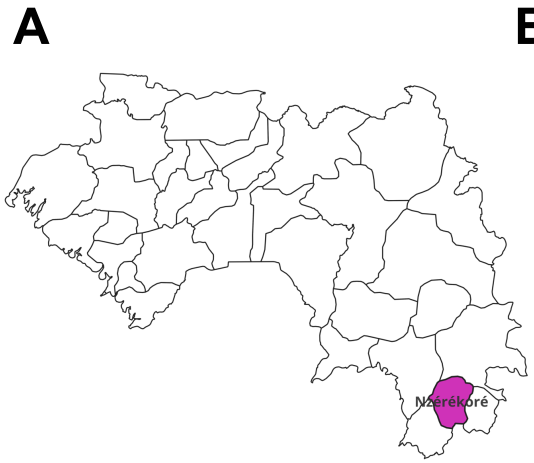

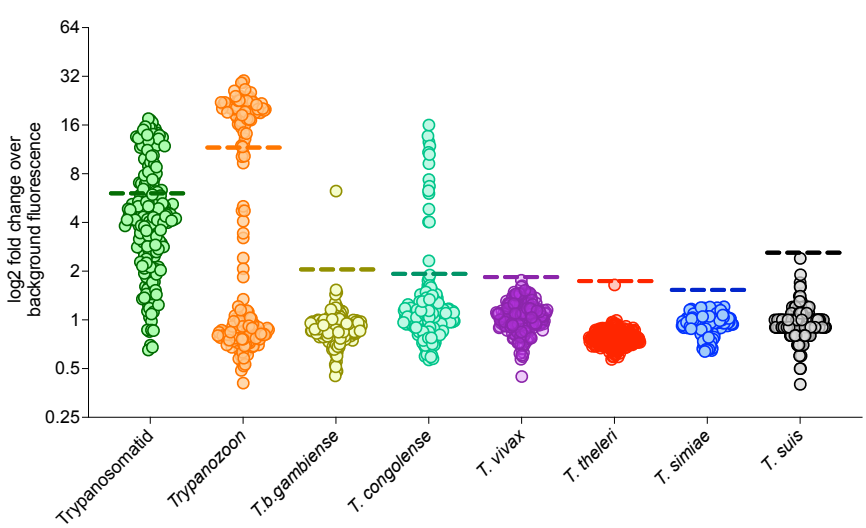

C

	No. positive samples	% infections (n=200)
Trypanosomatid	59	29.5 %
Trypanozoon	78	39.0 %
T. b. gambiense	1	0.50 %
T. congolense	15	7.5 %
T. vivax	0	0.0 %
T. theileri	0	0.0 %
T. simiae	0	0.0 %
T. suis	0	0.0 %

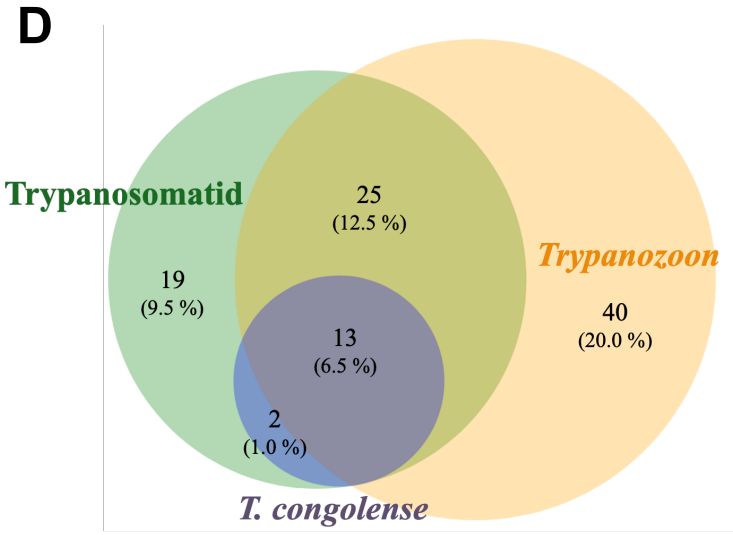

Supplementary Figure 1

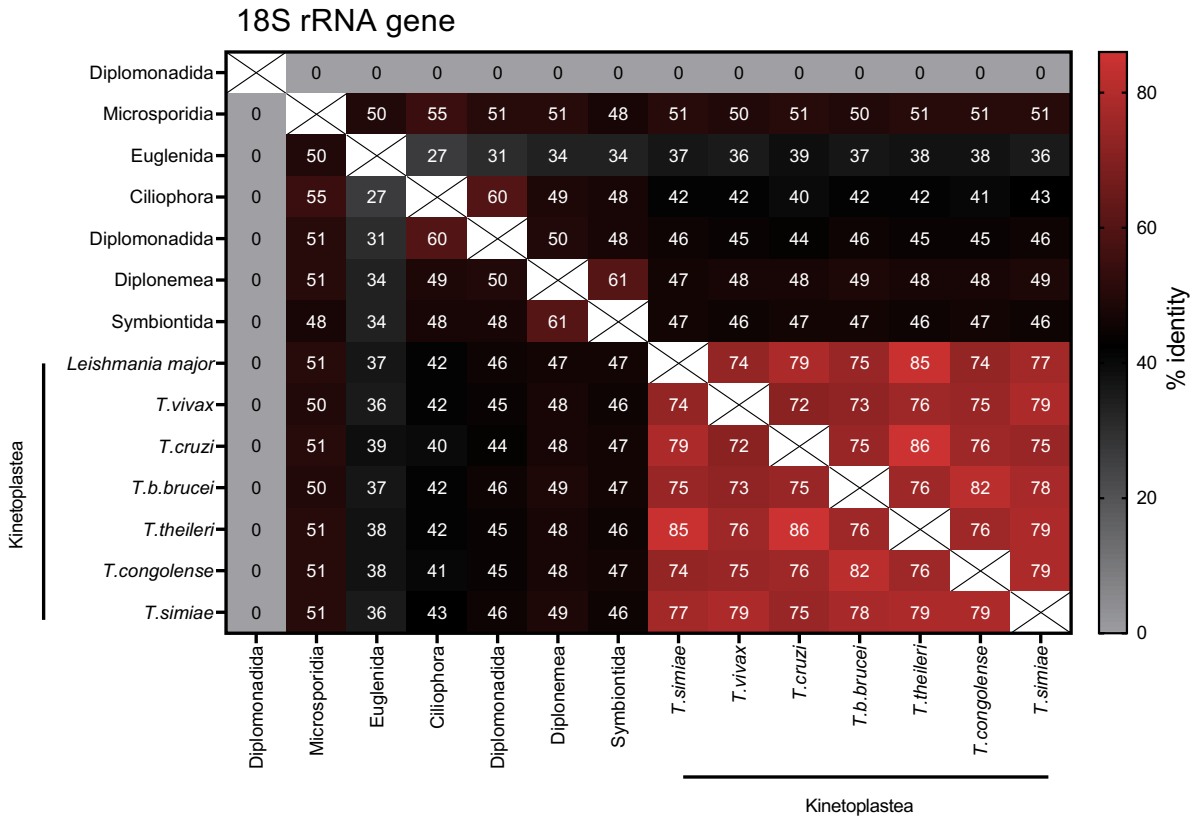

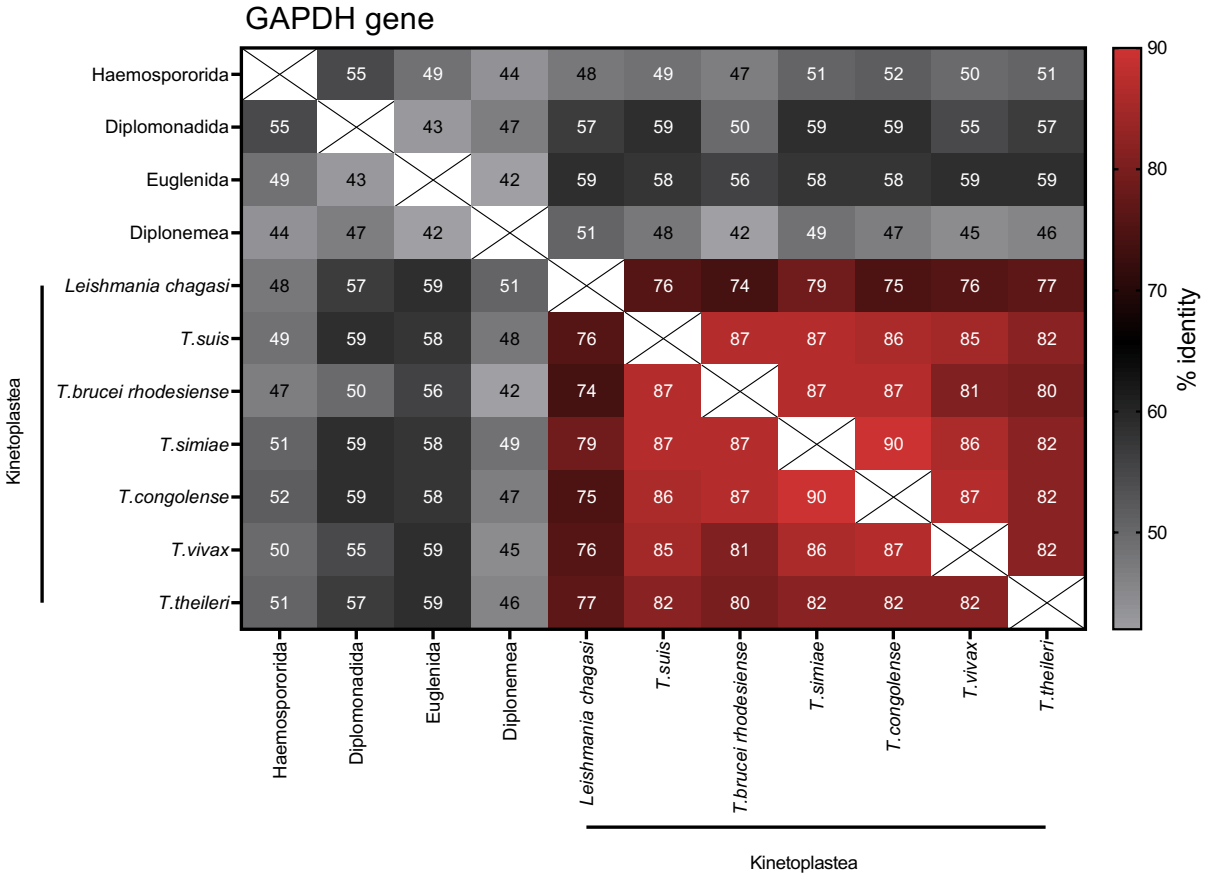

Supplementary Figure 2

A

```
                RPA Forward Primer          target region crRNA 1       target region crRNA 3    RPA Reverse Primer

Microsporidia   CTTAATTTGACTCAACGCGAGGTAA[…]AATATTTTATTATTCAGCGAGAATGGAA---[…]ATAGTGGTGCATGGGCCGTTTTCAATGGA TGCT-GTAAAGT-TTTGATTAATTTC
Ciliophora      CTTAATTTGACTCAACACTGGGAAA[…]AGGGCAAGAA---GATTTTAGGATTGACAGA[…]GTGGTGGTGCATGGCCGTTCTTAGC-TGG TGGA-GTGAGATGTCTGGTTAATTCC
Haemosporida    CTTAATTTGACTCAACACGGGAAAA[…]AGTTTAAGAC---AAGAGTAGGATTGACAGA[…]ATGGTGATGCATGGCCGTTTTTAGT-TCG TGAATATGATTTGTCTGGTTAATTCC
Diplomonadida   CTCAATCTGACTCAACGCGCG-CAC[…]AGGCCCGGAC---GCGCGGAGGACCGACAGC[…]GCGGTGGTGCATGGCCGCTCCCAGC-CCG TGGC-GCGAGCCGTCTGCTCCATTGC
Symbiontida     CTTAATTTGACTCAACACGGGAAAT[…]AGATCAGGAC---GCCCGGTGGATTGACAGA[…]ATGGTGGTGCATGGCCGCTCCTGGT-TGG TGGA-GTGATTTGTCTGGTTGATTCC
Diplonemea      CTTAATTTGACTCAACACGGGGAAT[…]AGGTCAGGAC---AATGTAAGGATTGACAGA[…]GTGGTGGTGCATGGCCGCTCCTGGT-TGG TGGA-GTGATTTGTCTGGTTGATTCC
Euglenida       CTTAATTTGACTCAACGCGGGGAAT[…]AGGTCCGGAC---GCAGCTGGGATGGACAGA[…]ACGGTGGTGCATGGCCGCTCCTGAT-TGG TGGA-GTGATTTGTCTGGTTGATTCC
Kinetoplastea   TTTAATTTGACTCAACACGGGGAAC[…]AGATCCGGAC---AGGGTGAGGATTGACAGA[…]ATGGTGGTGCATGGCCGCTTTTGGT-CGG TGGA-GTGATTTGTTTGGTTGATTCC
```

B

```
                    Forward RPA Primer          crRNA target region       Reverse RPA Primer

H, pdb|5VYC|i       ---------------------------[…]----------------------------[…]CCCGCCGGGCAGCTTC-------------
Pfl, XR_002966654.1 ------------------AAAATATAT[…]CATTTCTTAGGGAATGTTGATTTT----[…]TTCCTTCAGTACCTTA-------------
Lm, GQ332361.1      CCGCGCCCGCTTTTA---CCAACTTAC[…]TA----------TTCGGCCTTTAC----[…]TATCCTCAGCACGTTTTCTG--TTTTTTC
Tcz, AJ009147.1     TCTCGCCAATGAATATATTAAATTTAC[…]TT----------TTTGGTCTTCGTCTTT[…]TATCCTCAGCACGTTATCTGA-CTTCTTC
Tvx, EU477537.1     GCGCTCCACCAACCA--------TCAC[…]TTTGG-------CGCGGCCCTCGC----[…]TGTCCTCAGCACGTCC------AACCGCC
Tcg, AJ009146.1     GTGCAGTCACAACAA---ACAACTTAC[…]TGCTGCCGTACGTTCGCCCCTTATTTTT[…]TATCCTCAGCACGTTGTTTACATTTTTTC
Tth, AJ009163.1     CCTCGCCAATGGATA---TCAATTTAC[…]TT----------TTCGGTCCTCGC----[…]TATCCTCAGCACGTTATCTGA-CTTCTTC
Tsm, AJ404608.1     CCACAGCCAACTACA---CAAACTTAC[…]TGCCGCGGGTCGCC--------------[…]TATCCTCAGCACGTTGTTGA--CTCATTC
Tsu, MK954469.1     CGGTCCCAGTACTTA---ACAATTTAC[…]TTATATTCCGCCTGGCGTGCTTCGTTGT[…]TATCCTCAGCAC
Tbb, XR_002989632.1 GCCCCAATTTATTTA---TCAATTTAC[…]TATCACCCCCGGTTCCCTCTTTTGAGGT[…]TATCCTCAGCACGTTTCTTA--CTTCTTC
```

Supplementary Figure 3

BLAST exclusion	Range of amplicon percentage identity (arithmetic mean)	Number of sequences included	Percentage of sequences with conserved crRNA		Sequences with partially conserved crRNA	
			crRNA 1	crRNA 3	crRNA 1	crRNA 3
Family **Trypanosomatidae**	82.27 - 100% (98.4%)	1644	59.4 %	97.1 %	667	48
Order **Trypanosomatida**	82.27 - 100% (98.4%)	1652	59.6 %	97.1 %	667	48
Subclass **Metakinetoplastia**	81.88 – 100% (97.9%)	1931	57.6 %	94.8 %	818	100
Class **Kinetoplastea**	81.88 – 100% (97.3%)	2051	55.1 %	90.3 %	920	199
Phylum **Euglenozoa**	69.72 – 100% (91.7%)	3330	34.0 %	55.8 %	2199	1477
Phylum **Euglenozoa** (excluded Kinetoplastea)	69.72 – 98.55% (82.9%)	1287	0.6 %	0.7 %	1279	1278

Supplementary Figure 4

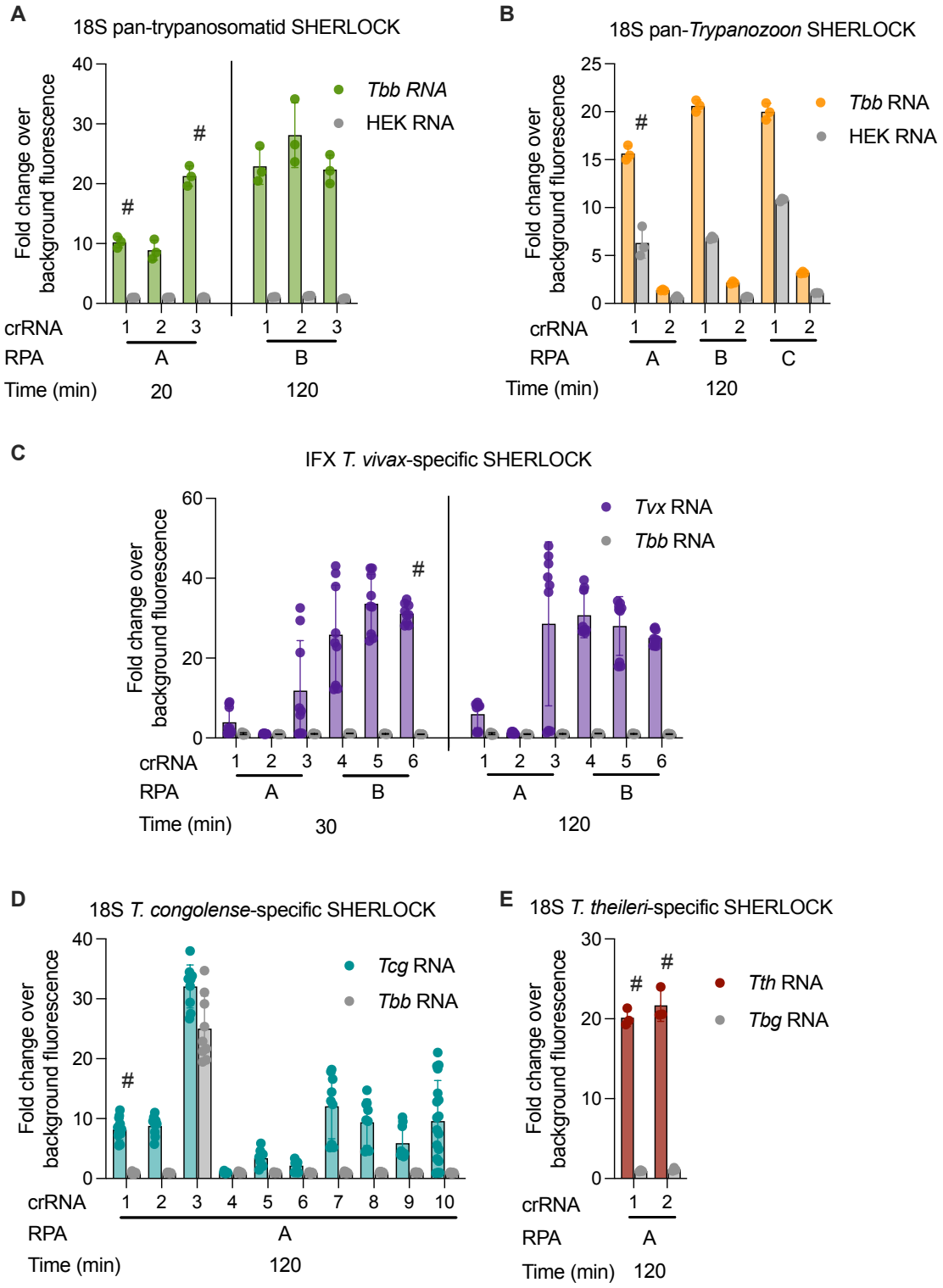

Supplementary Figure 5

	Accession	Alignment against the crRNA	Identity (%)	Query coverage
T. simiae	KR024686.1	TCCCTGCTCCGGCGGCGGGGCGACTCGC	90.62	100%
	KP307021.1	TCCCTGCTCCGGCGGCGGGGCGACTCGC	90.62	100%
	AJ009162.1	TCCCTGCTCCGGCGGCGGGGCGACTCGC	90.62	100%
	AJ223569.1	TCCCTGCTCCGGCGGCGGGGCGACTCGC	90.62	100%
	U22320.1	TCCCTGCTCCGGCGGCGGGGCGACTCGC	90.62	100%
	KP307022.1	TCCCTGCTCCGGCGGCGGGGCAACTCGC	89.06	100%
	AJ404608.1	TCCCTACCTCGGCGGCGGGGCAACTCGC	86.72	100%
	U22318.1	TCCCTACCTCGGCGGCGGGGCAACTCGC	86.72	100%
T. godfreyi	AJ009155.1	TCCCTACCCCGGCGGCGGGGCGACTCGC	88.28	100%
T. sapaensis	AB242822.1	TCTCTGTTCCGGCTGCGGGGCAACTCGT	88.28	100%
Trypanosoma vivax	EU477537.1	TCCCTGCTCCGGCGGCGGGGCAACCCGC	87.50	100%
	KM391829.1	TCCCTGCTCCGGCGACGGGGCAACCCGC	84.38	100%
	KM391828.1	TCCCTGCTCCGGCGACGGGGCAACCCGC	84.38	100%
	KM391827.1	TCCCTGCTCCGGCGACGGGGCAACCCGC	84.38	100%
	KM391826.1	TCCCTGCTCCGGCGACGGGGCAACCCGC	84.38	100%
	KM391823.1	TCCCTGCTCCGGCGACGGGGCAACCCGC	84.38	100%
	KM391822.1	TCCCTGCTCCGGCGACGGGGCAACCCGC	84.38	100%
	HE573019.1	TCCCTGCTCCGGCGACGGGGCAACCCGC	84.38	100%
	U22316.1	TCCCTGCTCCGGCGACGGGGCAACCCGC	84.13	98%
	KM391825.1	TCCCTGCTCCGGCGACGGCTTCCACCGC	83.59	100%
	KM391824.1	TCCCTGCTCCGGCGACGGCTTCCACCGC	83.59	100%
	KM391821.1	TCCCTGCTCCGGCGACGGCTTCCACCGC	83.59	100%
	KM391820.1	TCCCTGCTCCGGCGACGGCTTCCACCGC	83.59	100%
	KM391818.1	TCCCTGCTCCGGCGACGGCTTCCACCGC	83.59	100%
	KM391816.1	TCCCTGCTCCGGCGACGGCTTCCACCGC	83.59	100%
	KM391819.1	TCCCTGCTCCGGCGACGGCTTCCACCGC	82.81	100%
T. theileri	KR024688.1	TCTCTGTTCCGGCGGTGGGGCAACTCAC	86.72	100%
	LC618031.1	TCTCTGTTCCGGCGGTGGGGCAACTCAC	86.72	100%
	AJ009163.1	TCTCTGTTCCGGCGGTGGGGCAACTCAC	86.72	100%
	AB007814.1	TCTCTGTTCCGGCGGTGGGGCAACTCAC	86.72	100%
	LC618030.1	TCTCTGTTCCGGCGGTGGGGCAACTCAC	85.94	79%
	JX178191.1	TCTCTGTTCCGGCGGTGGGGCAACTCAC	85.29	79%
	JX178190.1	TCTCTGTTCCGGCGGTGGGGCAACTCAC	84.31	79%
	MG255951.1	TCTCTGTTACGGCGGTGGGGCAACTCAC	85.42	75%
	MG255958.1	TCTCTGTTCCGGCGGTGGGGCAACTCAC	84.38	75%
Trypanosoma thomasbancrofti	KT728394.1	TCTCTGTTCCGGCGGTGGGGCAACTCAC	85.94	100%
	KT728393.1	TCTCTGTTCCGGCGGTGGGGCAACTCAC	85.94	100%
	KT728392.1	TCTCTGTTCCGGCGGTGGGGCAACTCAC	85.94	100%
	KT728391.1	TCTCTGTTCCGGCGGTGGGGCAACTCAC	85.94	100%
	KT728390.1	TCTCTGTTCCGGCGGTGGGGCAACTCAC	85.94	100%
	KT728389.1	TCTCTGTTCCGGCGGTGGGGCAACTCAC	85.94	100%
	KT728388.1	TCTCTGTTCCGGCGGTGGGGCAACTCAC	85.94	100%
	KT728387.1	TCTCTGTTCCGGCGGTGGGGCAACTCAC	85.94	100%
	KT728386.1	TCTCTGTTCCGGCGGTGGGGCAACTCAC	85.94	100%
	KT728385.1	TCTCTGTTCCGGCGGTGGGGCAACTCAC	85.94	100%
	KT728384.1	TCTCTGTTCCGGCGGTGGGGCAACTCAC	85.94	100%
	KT728383.1	TCTCTGTTCCGGCGGTGGGGCAACTCAC	85.94	100%
	KT728382.1	TCTCTGTTCCGGCGGTGGGGCAACTCAC	85.94	100%
	KT728381.1	TCTCTGTTCCGGCGGTGGGGCAACTCAC	85.94	100%
	KT728380.1	TCTCTGTTCCGGCGGTGGGGCAACTCAC	85.94	100%
	KT728379.1	TCTCTGTTCCGGCGGTGGGGCAACTCAC	85.94	100%
	KT728378.1	TCTCTGTTCCGGCGGTGGGGCAACTCAC	85.94	100%
	KT728377.1	TCTCTGTTCCGGCGGTGGGGCAACTCAC	85.94	100%
	KT728376.1	TCTCTGTTCCGGCGGTGGGGCAACTCAC	85.94	100%
	KT728375.1	TCTCTGTTCCGGCGGTGGGGCAACTCAC	85.94	100%
	KT728374.1	TCTCTGTTCCGGCGGTGGGGCAACTCAC	85.94	100%
	KT728373.1	TCTCTGTTCCGGCGGTGGGGCAACTCAC	85.94	100%
	OM509729.1	TCTCTGTTCCGGCGGTGGGGCAACTCAC	85.94	100%
	KT728396.1	TCTCTGTTCCGGCGATGGGGCAACTCAC	84.38	100%
	KT728395.1	TCTCTGTTCCGGCGATGGGGCAACTCAC	84.38	100%
	crRNA 18STcg1	**TCCCTGCTACGGCCGCGGGGTGACTCGC**		

Supplementary Figure 6

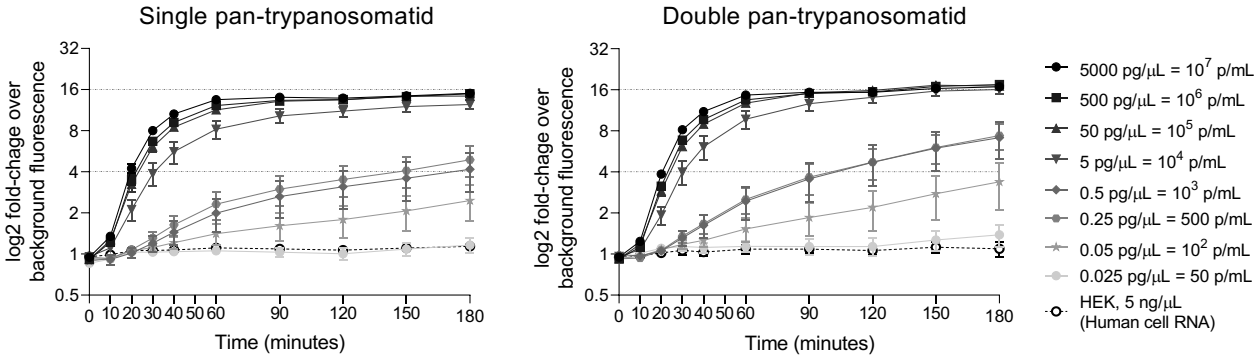

Supplementary Figure 7

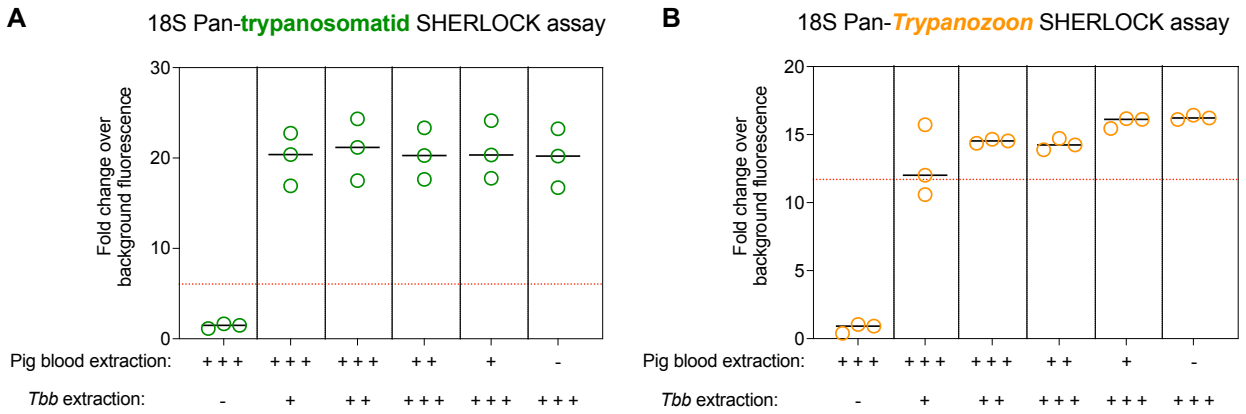

Supplementary Figure 8

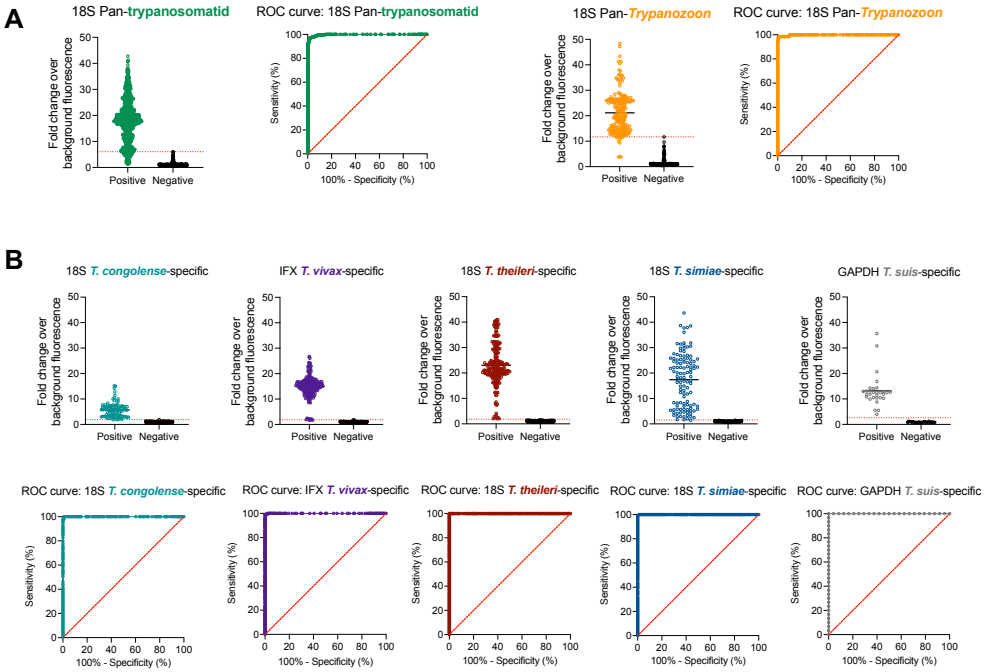

C

SHERLOCK Assay	Sensitivity (95 % CI)	Specificity (95 % CI)	Fold Change cut-off
Pan-trypanosomatid	**92.14 %** (90.43 to 93.57 %)	**100.0 %** (99.02 to 100.0 %)	**>6.050**
Pan-*Trypanozoon*	**95.10 %** (91.21 to 97.32 %)	**100.0 %** (97.93 to 100.0 %)	**>11.70**
T. vivax	**99.11 %** (96.82 to 99.84 %)	**100.0 %** (97.29 to 100.0 %)	**>1.831**
T. congolense	**97.98 %** (92.93 to 99.64 %)	**100.0 %** (97.04 to 100.0 %)	**>1.923**
T. theileri	**100.0 %** (98.42 to 100.0 %)	**100.0 %** (97.99 to 100.0 %)	**>1.805**
T. simiae	**99.12 %** (95.20 to 99.96 %)	**100.0 %** (96.60 to 100.0 %)	**>1.546**
T. suis	**100.0 %** (88.65 to 100.0 %)	**100.0 %** (86.20 to 100.0 %)	**>2.609**
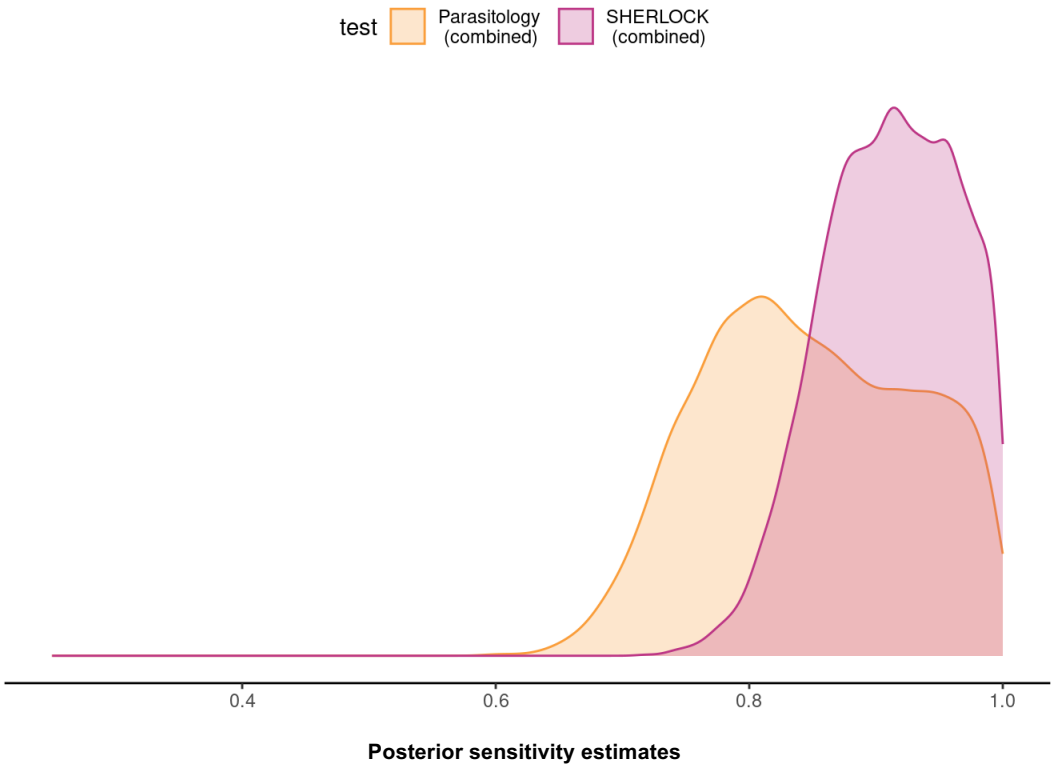
Supplementary Figure 9